Steel and Composite Structures, *Vol. 27, No. 3 (2018) 371-388*
DOI: https://doi.org/10.12989/scs.2018.27.3.371

Size dependent bending analysis of micro/nano sandwich structures based on a nonlocal high order theory

Omid Rahmani *, Soroush Deyhim and S. Amir Hossein Hosseini

Smart Structures and New Advanced Materials Laboratory, Department of Mechanical Engineering, University of Zanjan, Zanjan, Iran

(*Received January 7, 2017, Revised February 21, 2018, Accepted March 27, 2018*)

Abstract. In this paper, a new model based on nonlocal high order theory is proposed to study the size effect on the bending of nano-sandwich beams with a compliance core. In this model, in contrast to most of the available sandwich theories, no prior assumptions are made with respect to the displacement field in the core. Herein the displacement and the stress fields of the core are obtained through an elasticity solution. Equations of motion and boundary conditions for nano-sandwich beam are derived by using Hamilton's principle and an analytical solution is presented for simply supported nano-sandwich beam. The results are validated with previous studies in the literature. These results can be utilized in the study of nano-sensors and nano-actuators. The effect of nonlocal parameter, Young's modulus of the core and aspect ratio on the deflection of the nano-sandwich beam is investigated. It is concluded that by including the small-scale effects, the deflection of the skins is increased and by increasing the nonlocal parameter, the influence of small-scale effects on the deflections is increased.

Keywords: nano-sandwich; bending; high order theory; nonlocal theory

1. Introduction

Recently Nano materials have attracted the attention of scientific researcher's societies in fields such as engineering, physics and chemistry. Because of their Nano scale dimensions, Nano materials have unique properties. Nanoparticles, nanotubes, nanobeams and Nano plates are prevalent examples of these materials. Nano materials have special electrical, optical, chemical and mechanical properties and because of these advantageous properties, they are being utilized in nanostructures like Nano sensors, Nano electromechanical systems (NEMS), Nano-optomechanical systems (NOMS) and Nano composites (Eichenfield *et al*. (2009), Simsek 2011). To design these nanostructures with adequate precision, small-scale effects and atomic forces must be considered. Studies have shown that the small-scale effects significantly influence the mechanical properties in nanostructures. Ignoring these effects would lead to inaccurate designs. Small-scale effects can be considered in mechanical models via Eringen's nonlocal theory, which is a modified form of classical mechanics. Recently applying Eringen's nonlocal elasticity for analysis of nanostructures like nanobeams, Nano plates, carbon nanotubes, and graphene has been increased, because of its quick and reliable results (Murmu and Adhikari 2010, Rahmani 2014, Belkorissat *et al*. 2015, Jandaghian and Rahmani 2015, Bounouara *et al*. 2016). Nonlocal elasticity theory has been verified by experimental results in previous studies. Wang and Varadan (2006) studied vibration characteristic of both single-walled nanotubes (SWNTs) and double-walled nanotubes (DWNTs) via the nonlocal continuum mechanics and elastic beam theories. They denoted that the results of the nonlocal continuum mechanics are in reasonable agreement with the published experimental reports. Miandoab *et al*. (2015) used nonlocal elasticity theory to study the static behavior of electrically actuated micro and nano-beams. In this research free end gap of microbeam was compared with experimental results for different applied voltages. In addition, pull-in voltages are compared with experimental ones. As can be seen in results, nonlocal continuum theory reduces the difference between experimental and classical numerical results.In another study which was conducted by Patti *et al*. (2015) the flexural behavior of polypropylene composites filled with various contents of multi-wall carbon nanotube was assessed by experimental tests and modeled by using a nonlocal approach. Ghavanloo and Fazelzadeh (2013) developed nonlocal continuum based model to study the radial vibration of the anisotropic nanoparticles. The obtained results were successfully compared to experimental results for several nanoparticles including gold, silver, germanium, and cadmium selenide nano-particles. Moreover, it was observed that the frequency decreases with increasing nonlocal parameter, and the effect of nonlocal parameter on the frequency was significant for the nanoparticles with small radius.

There are various studies in the literature regarding the analysis of single nanobeams by utilizing nonlocal elasticity (Chaht *et al*. 2015, Jandaghian and Rahmani 2015, Pourseifi *et al*. 2015, Ahouel *et al*. 2016, Bounouara *et al*. 2016, Hayati *et al*. 2016, Hosseini and Rahmani 2016). Reddy (2007) rewrote the formulations of Euler-Bernoulli, Timoshenko, Reddy, and Levinson beam theories by using

*Corresponding author, Ph.D.,
E-mail: omid.rahmani@znu.ac.ir

http://www.techno-press.org/?journal=scs&subpage=6

ISSN: 1229-9367 (Print), 1598-6233 (Online)

Eringen’s nonlocal elasticity and obtained the governing equations of the nonlocal theories. Analytical solutions were shown for bending, buckling and vibration by utilizing the nonlocal theories and the influence of nonlocal parameter on deflections, buckling loads, and natural frequencies were determined. Emam (2013) exhibited a nonlocal nonlinear model for buckling of nanobeams. This model is appropriate for Euler-Bernoulli, Timoshenko, and higher-order shear deformation beam theories. The nonlocal effects were modeled based on Eringen’s nonlocal theory. Analytical solutions for the critical buckling load were shown and the influence of nonlocal effects and aspect ratio on critical buckling load and the amplitude of buckling for simply supported and fixed-fixed nanobeams were investigated. Nguyen *et al*. (2014) present an analytical solutions for the size-dependent static analysis of the functionally graded (FG) nanobeams with various boundary conditions based on the nonlocal continuum model. Zemri *et al*. (2015) present a nonlocal shear deformation beam theory for bending, buckling and vibration of functionally graded nanobeams by using the nonlocal differential constitutive relations of Eringen. A new nonlocal hyperbolic refined plate model for free vibration properties of functionally graded (FG) plates was presented by Belkorissat *et al*. (2015). This nonlocal nano-plate model incorporates the length scale parameter which can capture the small scale effect. Shojaeefard *et al*. (2018) studied the free vibration of a rotating variable thickness two-directional FG circular microplate. The results revealed that there was a non-proportional relation between the natural frequencies of the microplate and the thickness-variations of the section. The results showed that the increase of the size dependency would lead to the reduction of the non-dimensional natural frequency as well as the critical angular velocity. In another study, they investigated free vibration and thermal buckling of micro temperature-dependent FG porous circular plate subjected to a nonlinear thermal load. The results reveal that the increase of size dependency and the temperature-change would lead to the increase of differences between the first natural frequencies predicted based on the two theories (Shojaeefard *et al*. 2017). Najafi *et al*. (Najafi *et al*. 2017) studied the nonlinear dynamic response of FGM beams with Winkler–Pasternak foundation subject to noncentral low velocity impact in thermal field. In this paper also by using a modified Hertz’s contact law, the influence of material properties of the substrate layers on impact response and a general case of impact with different indenter’s axial position was taken into account. In another study, they presented (Najafi *et al*. 2016) a nonlinear analysis for impact response of functionally graded material plates which are resting on a nonlinear three-parameter elastic foundation with simply supported end condition. The effect of thermal field was considered and material properties of the plates were assumed to be temperature dependent.

Extensive studies have been conducted regarding the analysis of sandwich structures with soft cores (Phan *et al*. 2012a, b, Rahmani *et al*. 2012, Frostig *et al*. 2013, Frostig 2014, Khalili *et al*. 2014, Bennai *et al*. 2015, Bouchafa *et al*. 2015, Hamidi *et al*. 2015, Yuan *et al*. 2015, Lashkari and Rahmani 2016). Phan *et al*. (2012a) investigated the bending of a sandwich beam with nonidentical skins and a vertically flexible core by using high-order theory which is based on Hamilton’s principle. In this theory, it is assumed that horizontal and vertical displacements in the core are nonlinear. The Analysis utilized classical beam theory for the skins and a two-dimensional elasticity theory for the core.

Recently limited studies regarding nano-sandwich beams/plates consisting of two single nanobeams/ nanoplates and a soft core have been conducted (Hosseini and Rahmani 2016, Rahmani *et al*. 2016). Analysis of nano-sandwich beams and plates are very beneficial because of their applications in NEMS, NOMS, nano composites and nano sensors (Murmu and Adhikari 2010, 2011a, b, Murmu *et al*. 2011). Murmu and Adhikari (2011a) investigated the buckling of double-nanobeam-systems. These systems were modeled by Eringen’s nonlocal elasticity. The effect of nonlocal parameter on buckling and effect of stiffness of elsatic medium between two nanobeams on nonlocal parameter were investigated. Murmu *et al*. (2011) studied the buckling behavior of bonded double-nanoplate-systems. Thesmall-scale effects were included in the analysis by using Eringen’s nonlocal elasticity. An analytical method was used to obtain the buckling load of a double-nanoplate-system. The influnce of nonlocal effects on buckling of the double-nanoplate-system and effect of stiffness of the elastic medium between two nanoplates on nonlocal parameter were studied. Murmu and Adhikari (2010) studied the nonlocal transverse vibration of double-nanobeam-systems. Expressions for free vibration of these systems were developed by using Eringen’s nonlocal elasticity. The effect of nonlocal parameter on natural frequencies and effect of stiffness of elsatic medium between two nanobeams on nonlocal parameter were studied. Murmu and Akhikari (2011b) also investigated the nonlocal vibration of bonded double-nanoplate-systems. Expression for free vibration of double-nanoplate-systems were obtained using nonlocal elasticity. An analytical method was used for obtaining the natural frequencies of double-nanoplate-system. The influence of nonlocal effects on natural frequencies of the double-nanoplate-system and the effect of stiffness of the elastic medium between two nanoplates on nonlocal parameter were investigated.

In this paper, bending analysis of nano-sandwich beams is investigated by using high-order and nonlocal theories. The presented model is consisted of a transversely flexible core and two thin skins. It is assumed that the skins are linearly elsatic and the core is a two dimensional medium which has shear resistance and nonlinear displacement fileds and is completely connected to the skins. It is assumed that the longitudinal stresses of the core are negligible, since flexibility of the core is extremely higher than the skins. Equations of motion are derived by using high-order and nonlocal theories. Differential equations for bending of a simply-supported nano-sandwich beam are solved and numerical results are obtained. The effects of nonlocal parameter, stiffness of the core and length to height ratio on deflection of the nano-sandwich beam are studied.

2. Nonlocal elasticity

In Eringen's nonlocal theory, it is assumed that the stress field at a point x in an elastic body which is dependent on the strain field at that point is also dependent on strain fields at all other points in the body. Nonlocal stress tensor σ at point x can be expressed as

$$\sigma = \int_V R(|x' - x|, \eta)\sigma'(x')dx' \tag{1}$$

Where $\sigma'(x)$ is the classic stress tensor at point x and the function $R(|x'-x|, \eta)$ corresponds to the nonlocal modulus; $|x'-x|$ is the distance and η is a material constant depending on internal and external characteristic lenghts (e.g., lattice spacing and wavelength, respectively). According to Hooke's law, the stress σ' at the point x is dependent on the strain ε at that point

$$\sigma'(x) = D(\mathrm{x}) : \varepsilon(\mathrm{x}) \tag{2}$$

where D is the elasticity tensor, and : is the double-dot product.

Eqs. (1)-(2) together define the nonlocal constitutive relation for a Hookean continuum. Solving the elasticity problems by using Eq. (1) has proven to be a difficult task, because of its integral form. Thus, to simplify the process, an equivalent differential form was introduced. This differential relation is expressed as

$$(1 - \eta^2 l^2 \nabla^2)\sigma = \sigma', \quad \eta = \frac{e_0 a}{l} \tag{3}$$

where e_0 is a material constant and a and l are the internal and external characteristic lengths, respectively.

By using Eqs. (2)-(3), stress resultants can be expressed in terms of strains. Unlike in local theory where relations between stress resultants and strains can be expressed by linear algebraic equations, nonlocal theory expresses these relations by differential equations. For homogeneous isotropic beams with the assumption that the nonlocal behavior is insignificant in thickness direction, the nonlocal constitutive relation in Eq. (3) takes the following forms

$$\sigma_{xx} - \mu\sigma_{xx,xx} = E\,\varepsilon_{xx}, \quad \tau - \mu\tau_{,xx} = G\gamma_{xz} \quad \left[\mu = (e_0 a)^2\right] \tag{4}$$

where E and G are Young's modulus and shear modulus, respectively; μ is called the nonlocal parameter; The x-coordinate and z-coordinate are taken along the length and thickness of the beam, respectively, and$y$-coordinate is taken along the width of the beam; σ_{xx} and ε_{xx} are longitudinal stress and strain, respectively, andτ and$\gamma_{xz}$are shear stress and strain, respectively; $(\quad)_{,xx}$ is the second derivative with respect to x-coordinate (Reddy 2007).

In-plane resultants for the beam are

$$N_{xx} = \int_A \sigma_{xx} dA, \quad M_{xx} = \int_A z\,\sigma_{xx} dA \tag{5}$$

where A is the area of the cross-section of the beam.

In all beam theories, the resultant axial force-strain relation is similar and it is given by

$$N_{xx} - \mu N_{\mathrm{xx},xx} = EAu_{0,\mathrm{x}} \tag{6}$$

where u_0 is the horizontal displacement of mid-plane of the beam, and $(\quad)_{,x}$ is the first derivative with respect to x-coordinate.

In Euler-Bernoulli beam theory, the relation between the resultant bending moment and strain is given by

$$M_{xx} - \mu M_{\mathrm{xx},xx} = -EIw_{,xx} \tag{7}$$

where w is the vertical displacement and I is the second moment of area about the y-axis (Reddy 2007).

3. Mathematical formulation

The governing equations, boundary and continuity conditions for a static nano-sandwich beam can be derived using Hamilton's principle. This method minimizes the total energy, as follows

$$\delta(U + V) = 0 \tag{8}$$

where U and V are the internal potential energy and external work, respectively. δ is the variational operator.

The relation of the variation of the internal potential energy in terms of stress and strain is

$$\delta U = \int_{v_{top}} \sigma_{xx}\delta\varepsilon_{xx} dv + \int_{v_{bot}} \sigma_{xx}\delta\varepsilon_{xx} dv + \int_{v_{core}} \sigma_{zz}\delta\varepsilon_{zz} dv + \int_{v_{core}} \tau_c \delta\gamma_c dv \tag{9}$$

where σ_{xx} and ε_{xx} are the longitudinal stresses and strains in the upper and lower skins; τ_c and γ_c are shear stresses and strains in the core; σ_{zz} and ε_{zz} are the vertical stresses and strains in the core; v_{top}, v_{bot} and v_{core} are the volume of the top and bottom skins and the core, respectively; dv is the differential volume.

The relation of the variation of the external work is

$$\delta V = -\int_0^l (n_t\delta u_t + n_b\delta u_b + q_t\delta w_t + q_b\delta w_b + m_t\delta w_{t,x} + m_b\delta w_{b,x})dx \tag{10}$$

where n_i, q_i, and m_i ($i = t$, b) are the distributed horizontal, vertical loads, and bending moments, respectively, which are applied to top and bottom skins; u_i, w_i, and $w_{i,x}$ ($i = t$, b) are the horizontal, vertical displacement, and rotation in the skins, respectively; dx is the differential length. The geometry of the nano-sandwich beam is shown in Fig. 1.

According to Euler-bernoulli beam theory, strain-displacement relations for the skins are

$$\varepsilon_{xx}^t = u_{0t,x} - z_t w_{\mathrm{t,xx}} \tag{11a}$$

$$\varepsilon_{xx}^b = u_{0b,x} - z_b w_{b,xx} \tag{11b}$$

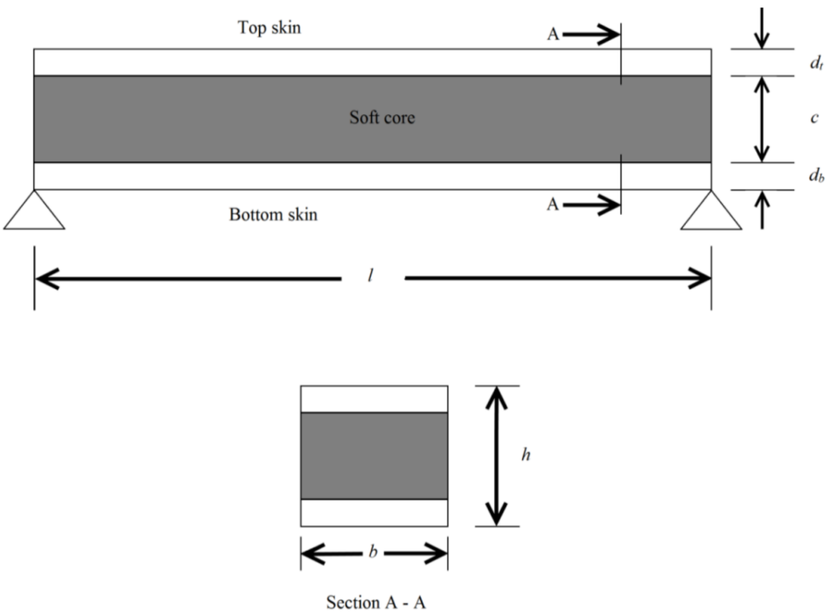

Fig. 1 Geometry of the nano-sandwich beam

where z_i (i = t, b) is the vertical coordinate of each skin, which is measured downward from neutural axis of each skin.

Strain-displacement relations for the core are

$$\gamma_c = u_{c,z} + w_{c,x} \tag{12a}$$

$$\varepsilon_{zz} = w_{c,z} \tag{12b}$$

where u_c and w_c are the horizontal and vertical displacements in the core, respectively; z is the vertical coordinate of the core, which is measured downward from the upper interface; $(\quad)_{,z}$ is the first derivative with respect to z-coordinate.

Continuity conditions for the upper and lower interfaces are

At $z = 0$

$$u_c^t = u_{0t} - \frac{d_t}{2} w_{t,x} \tag{13a}$$

$$w_c^t = w_t \tag{13b}$$

At $z = c$

$$u_c^b = u_{0b} + \frac{d_b}{2} w_{b,x} \tag{14a}$$

$$w_c^b = w_b \tag{14b}$$

where u^i_c and w^i_c (i = t, b) are the longitudinal and vertical displacements in the core at the interfaces, respectively; d_i (i = t, b) and c are the thickness of skins, and the core, respectively (Frostig *et al*. 1992).

Equations of motion can be derived by substituting Eqs. (9)-(10) in Eq. (8), by using strain-displacement relations (Eqs. (11)-(12)) and integration by parts, and with the use of continuity conditions (Eqs. (13)-(14))

$$N^t_{xx,x} + b\,\tau_c\big|_{z=0} + n_t = 0 \tag{15}$$

$$N^b_{xx,x} - b\,\tau_c\big|_{z=c} + n_b = 0 \tag{16}$$

$$M^t_{xx,xx} + \frac{bd_t}{2}\tau_{c,x}\big|_{z=0} + b\,\sigma_{zz}\big|_{z=0} + q_t - m_{t,x} = 0 \tag{17}$$

$$M^b_{xx,xx} + \frac{bd_b}{2}\tau_{c,x}\big|_{z=c} - b\,\sigma_{zz}\big|_{z=c} + q_b - m_{b,x} = 0 \tag{18}$$

$$\tau_{c,x} + \sigma_{zz,z} = 0 \tag{19}$$

$$\tau_{c,z} = 0 \tag{20}$$

where N^i_{xx} and M^i_{xx} (i = t, b) are the in-plane resultants of the skins, respectively, and b is the width of the beam.

According to Eq. (20) the shear stress τ_c is only a function of x-coordinate. Therefore

$$\tau_c\big|_{z=0} = \tau_c\big|_{z=c} = \tau(x) \tag{21}$$

According to Eqs. (6)-(7), constitutive relations for the skins of the nano-sandwich beam are ($i = t$, b)

$$N^i_{xx} - \mu N^i_{xx,xx} = E_i A_i u_{0i,x} \tag{22}$$

$$M^i_{xx} - \mu M^i_{xx,xx} = -E_i I_i w_{i,xx} \tag{23}$$

and also, according to Eq. (4), constitutive relations for the core of the nano-sandwich beam are

$$\tau - \mu\tau_{,xx} = G_c\gamma_c \tag{24}$$

$$\sigma_{zz} - \mu\sigma_{zz,zz} = E_c\varepsilon_{zz} \tag{25}$$

where E_c and G_c are Young's modulus and shear modulus of the core, respectively.

According to Eqs. (19)-(21), $\sigma_{zz,zz}$ in Eq. (25) will be zero. Thus

$$\sigma_{zz} = E_c\varepsilon_{zz} \tag{26}$$

The vertical and horizontal displacements in the core can be determined by using Eqs. (19)-(24). By integrating Eq. (19) with respect to z, the following relation is acquired

$$\sigma_{zz}(x,z) = -\tau_{,x}z + c_1 \tag{27}$$

Vertical displacement in the core (w_c) is obtained by substituting σ_{zz} from Eq. (26) into Eq. (27), by using Eq. (12b) and integrating with respect to z along the height of the core, and by using the continuity condition at the upper and lower interface layers

$$w_c = \frac{-\tau_{,x}}{2E_c}z^2 + \left(\frac{w_b - w_t}{c} + \frac{\tau_{,x}c}{2E_c}\right)z + w_t \tag{28}$$

Also, the vertical stress in the core takes the following form

$$\sigma_{zz} = -\tau_{,x}z + \frac{E_c(w_b - w_t)}{c} + \frac{\tau_{,x}c}{2} \tag{29}$$

According to Eq. (24), the shear strain in the core is

$$\gamma_c = \frac{1}{G_c}(\tau - \mu\tau_{,xx}) \tag{30}$$

By substituting γ_c from Eq. (12a) into Eq. (30), the following relation is obtained

$$u_{c,z} = \frac{1}{G_c}(\tau - \mu\tau_{,xx}) - w_{c,x} \tag{31}$$

Horizontal displacement in the core (u_c) is acquired by substituting w_c from Eq. (28) into Eq. (31), and integrating with respect to z along the height of the core, and by utilizing the continuity condition at the upper interface layer

$$\begin{aligned} u_c = {} & \frac{1}{G_c}(\tau - \mu\tau_{,xx})z + \frac{\tau_{,xx}}{6E_c}z^3 - \frac{w_{b,x}}{2c}z^2 \\ & - \frac{\tau_{,xx}c}{4E_c}z^2 + \left(\frac{z^2}{2c} - z - \frac{d_t}{2}\right)w_{t,x} + u_{0t} \end{aligned} \tag{32}$$

The governing equations for the nano-sandwich beam are formulated with the use of five unknowns: u_{0t}, u_{0b}, w_t, w_b, and τ. Four of the governing equations are derived by substituting N^i_{xx}, M^i_{xx}, τ, and σ_{zz} from Eqs. (22)-(24), (29) into Eqs. (15)-(18), and then again by using Eqs. (15)-(18). The fifth governing equation is obtained by applying continuity condition at the lower interface layer to Eq. (32). The governing equations are as follows

$$\begin{aligned} & \left(E_tA_tu_{0t,x}\right)_{,x} + b(\tau - \mu\tau_{,xx}) + n_t \\ & -\mu n_{t,xx} = 0 \end{aligned} \tag{33}$$

$$\begin{aligned} & \left(E_bA_bu_{0b,x}\right)_{,x} - b(\tau - \mu\tau_{,xx}) + n_b \\ & -\mu n_{b,xx} = 0 \end{aligned} \tag{34}$$

$$\begin{aligned} & \left(E_tI_tw_{t,xx}\right)_{,xx} \\ & -\frac{bE_c}{c}\left(w_b - w_t - \mu(w_{b,xx} - w_{t,xx})\right) \\ & -\frac{b(c+d_t)}{2}\left(\tau_{,x} - \mu\tau_{,xxx}\right) \\ & -q_t + \mu q_{t,xx} + m_{t,\mathrm{x}} - \mu m_{t,xxx} = 0 \end{aligned} \tag{35}$$

$$\begin{aligned} & \left(E_bI_bw_{\mathrm{b},xx}\right)_{,xx} \\ & +\frac{bE_c}{c}\left(w_b - w_t - \mu(w_{b,xx} - w_{t,xx})\right) \\ & -\frac{b(c+d_b)}{2}\left(\tau_{,x} - \mu\tau_{,xxx}\right) \\ & -q_b + \mu q_{\mathrm{b},xx} + m_{\mathrm{b,x}} - \mu m_{\mathrm{b},xxx} = 0 \end{aligned} \tag{36}$$

$$\begin{aligned} & u_{0b} - u_{0t} - \frac{c}{G_c}\tau + \left(\frac{\mu c}{G_c} + \frac{c^3}{12E_c}\right)\tau_{,xx} \\ & + \frac{(c+d_b)}{2}w_{b,x} + \frac{(c+d_t)}{2}w_{t,x} = 0 \end{aligned} \tag{37}$$

With the use of Eq. (37), τ can be eliminated from the governing equations. By doing so, the number of governing equations and the unknowns will be reduced to four. These four governing equations are as follows

$$\begin{aligned} & \frac{c}{G_c}E_tA_tu_{0t,xx} - \left(\frac{\mu c}{G_c} + \frac{c^3}{12E_c}\right)E_tA_tu_{0t,xxxx} \\ & +b\left(u_{0b} - u_{0t} + \frac{(c+d_b)}{2}w_{b,x} + \frac{(c+d_t)}{2}w_{t,x}\right) \\ & -b\mu\left(\begin{aligned} & u_{0b,xx} - u_{0t,xx} \\ & + \frac{(c+d_b)}{2}w_{b,xxx} + \frac{(c+d_t)}{2}w_{t,xxx} \end{aligned}\right) \end{aligned} \tag{38}$$

$$\begin{aligned} & \frac{c}{G_c}E_bA_bu_{0b,xx} - \left(\frac{\mu c}{G_c} + \frac{c^3}{12E_c}\right)E_bA_bu_{0b,xxxx} \\ & -b\left(u_{0b} - u_{0t} + \frac{(c+d_b)}{2}w_{b,x} + \frac{(c+d_t)}{2}w_{t,x}\right) \end{aligned} \tag{39}$$

$$
\begin{aligned}
&+b\mu\left(\begin{array}{l} u_{0b,xx}-u_{0t,xx} \\ +\frac{(c+d_b)}{2}w_{b,xxx}+\frac{(c+d_t)}{2}w_{t,xxx} \end{array}\right) \\
&+\frac{c}{G_c}n_b-\left(\frac{2\mu c}{G_c}+\frac{c^3}{12E_c}\right)n_{b,xx} \\
&+\mu\left(\frac{\mu c}{G_c}+\frac{c^3}{12E_c}\right)n_{b,xxxx}=0
\end{aligned} \tag{39}
$$

$$
\begin{aligned}
&\frac{c}{G_c}E_tI_tw_{t,xxxx}-E_tI_t\left(\frac{\mu c}{G_c}+\frac{c^3}{12E_c}\right)w_{t,xxxxxx} \\
&+\frac{b\mu E_c}{G_c}\left(w_{b,xx}-w_{t,xx}\right) \\
&-\frac{b\mu E_c}{c}\left(\frac{\mu c}{G_c}+\frac{c^3}{12E_c}\right)\left(w_{b,xxxx}-w_{t,xxxx}\right) \\
&+\frac{b\mu(c+d_t)}{2}\left(\begin{array}{l} u_{0b,xxx}-u_{0t,xxx} \\ +\frac{(c+d_b)}{2}w_{b,xxxx} \\ +\frac{(c+d_t)}{2}w_{t,xxxx} \end{array}\right) \\
&-\frac{c}{G_c}q_t+\left(\frac{2\mu c}{G_c}+\frac{c^3}{12E_c}\right)q_{t,xx} \\
&-\mu\left(\frac{\mu c}{G_c}+\frac{c^3}{12E_c}\right)q_{t,xxxx} \\
&+\frac{c}{G_c}m_{t,x}-\left(\frac{2\mu c}{G_c}+\frac{c^3}{12E_c}\right)m_{t,xxx} \\
&+\mu\left(\frac{\mu c}{G_c}+\frac{c^3}{12E_c}\right)m_{t,xxxxx} \\
&-\frac{b(c+d_t)}{2}\left(\begin{array}{l} u_{0b,x}-u_{0t,x} \\ +\frac{(c+d_b)}{2}w_{b,xx} \\ +\frac{(c+d_t)}{2}w_{t,xx} \end{array}\right) \\
&-\frac{bE_c}{G_c}\left(w_b-w_t\right) \\
&+\frac{bE_c}{c}\left(\frac{\mu c}{G_c}+\frac{c^3}{12E_c}\right)\left(w_{b,xx}-w_{t,xx}\right)=0
\end{aligned} \tag{40}
$$

$$
\begin{aligned}
&\frac{c}{G_c}E_bI_bw_{b,xxxx}-E_bI_b\left(\frac{\mu c}{G_c}+\frac{c^3}{12E_c}\right)w_{b,xxxxxx} \\
&-\frac{b\mu E_c}{G_c}\left(w_{b,xx}-w_{t,xx}\right) \\
&+\frac{b\mu E_c}{c}\left(\frac{\mu c}{G_c}+\frac{c^3}{12E_c}\right)\left(w_{b,xxxx}-w_{t,xxxx}\right) \\
&+\frac{b\mu(c+d_b)}{2}\left(\begin{array}{l} u_{0b,xxx}-u_{0t,xxx} \\ +\frac{(c+d_b)}{2}w_{b,xxxx} \\ +\frac{(c+d_t)}{2}w_{t,xxxx} \end{array}\right) \\
&-\frac{c}{G_c}q_b+\left(\frac{2\mu c}{G_c}+\frac{c^3}{12E_c}\right)q_{b,xx} \\
&-\mu\left(\frac{\mu c}{G_c}+\frac{c^3}{12E_c}\right)q_{b,xxxx} \\
&+\frac{c}{G_c}m_{b,x}-\left(\frac{2\mu c}{G_c}+\frac{c^3}{12E_c}\right)m_{b,xxx} \\
&+\mu\left(\frac{\mu c}{G_c}+\frac{c^3}{12E_c}\right)m_{b,xxxxx} \\
&-\frac{b(c+d_b)}{2}\left(\begin{array}{l} u_{0b,x}-u_{0t,x} \\ +\frac{(c+d_b)}{2}w_{b,xx} \\ +\frac{(c+d_t)}{2}w_{t,xx} \end{array}\right) \\
&+\frac{bE_c}{G_c}\left(w_b-w_t\right) \\
&-\frac{bE_c}{c}\left(\frac{\mu c}{G_c}+\frac{c^3}{12E_c}\right)\left(w_{b,xx}-w_{t,xx}\right)=0
\end{aligned} \tag{41}
$$

It is assumed that the nano-sandwich beam is simply-supported at the lower skin and is free at the upper skin, and is under the load q_t, which is applied to the upper skin. Therefore, for solving the governing equations for this nano-sandwich beam, Navier's method is utilized. According to this method, u_{0t}, u_{0b}, w_t, w_b, and q_t are expressed as

$$u_{0t}=\sum_{i=1}^{\infty}C_{ut}(i)\cos\left(\frac{i\pi x}{l}\right) \tag{42}$$

$$u_{0b}=\sum_{i=1}^{\infty}C_{ub}(i)\cos\left(\frac{i\pi x}{l}\right) \tag{43}$$

$$w_t=\sum_{i=1}^{\infty}C_t(i)\sin\left(\frac{i\pi x}{l}\right) \tag{44}$$

$$w_b=\sum_{i=1}^{\infty}C_b(i)\sin\left(\frac{i\pi x}{l}\right) \tag{45}$$

$$
\begin{aligned}
q_t&=\sum_{i=1}^{\infty}\mathrm{Q}_i\sin\left(\frac{i\pi x}{l}\right) \\
Q_i&=\frac{2}{l}\int_0^l q_t\sin\left(\frac{i\pi x}{l}\right)dx
\end{aligned} \tag{46}
$$

where l is the length of the beam. Q_i for uniform load q_0, point load P (applied to $x = a$), and sinusoidal load $q_0 \sin(\pi x/l)$ is given below

$$\begin{aligned}
&q_t(x) = q_0 \quad \Leftrightarrow \quad Q_i = \frac{4q_0}{i\pi}, \quad i = 1,3,5,\ldots \\
&q_t(x) = P\delta(x-a) \\
&\Leftrightarrow \quad Q_i = \frac{2P}{l}\sin\left(\frac{i\pi a}{l}\right), \quad i = 1,2,3,\ldots \\
&q_t(x) = q_0 \sin\left(\frac{\pi x}{l}\right) \\
&\Leftrightarrow \quad Q_1 = q_0, \quad Q_i = 0, \quad i = 2,3,\ldots
\end{aligned} \tag{47}$$

Substituting u_{0t}, u_{0b}, w_t, w_b, and q_t from Eqs. (42)-(46) into Eqs. (38)-(41) yields

$$\begin{aligned}
&-\left[\begin{array}{l}\dfrac{c}{G_c}E_tA_t\left(\dfrac{i\pi}{l}\right)^2 \\ +\left(\dfrac{\mu c}{G_c}+\dfrac{c^3}{12E_c}\right)E_tA_t\left(\dfrac{i\pi}{l}\right)^4 \\ +b+b\mu\left(\dfrac{i\pi}{l}\right)^2\end{array}\right]C_{ut}(i) \\
&+\left[b+b\mu\left(\frac{i\pi}{l}\right)^2\right]C_{ub}(i) \\
&+\left[\begin{array}{l}\dfrac{b(c+d_t)}{2}\left(\dfrac{i\pi}{l}\right)+ \\ \dfrac{b\mu(c+d_t)}{2}\left(\dfrac{i\pi}{l}\right)^3\end{array}\right]C_t(i) \\
&+\left[\begin{array}{l}\dfrac{b(c+d_b)}{2}\left(\dfrac{i\pi}{l}\right) \\ +\dfrac{b\mu(c+d_b)}{2}\left(\dfrac{i\pi}{l}\right)^3\end{array}\right]C_b(i) = 0
\end{aligned} \tag{48}$$

$$\begin{aligned}
&-\left[\begin{array}{l}\dfrac{c}{G_c}E_bA_b\left(\dfrac{i\pi}{l}\right)^2 \\ +\left(\dfrac{\mu c}{G_c}+\dfrac{c^3}{12E_c}\right)E_bA_b\left(\dfrac{i\pi}{l}\right)^4 \\ +b+b\mu\left(\dfrac{i\pi}{l}\right)^2\end{array}\right]C_{ub}(i) \\
&+\left[b+b\mu\left(\frac{i\pi}{l}\right)^2\right]C_{ut}(i) \\
&-\left[\begin{array}{l}\dfrac{b(c+d_b)}{2}\left(\dfrac{i\pi}{l}\right) \\ +\dfrac{b\mu(c+d_b)}{2}\left(\dfrac{i\pi}{l}\right)^3\end{array}\right]C_b(i) = 0
\end{aligned} \tag{49}$$

$$\begin{aligned}
&-\left[\frac{b(c+d_t)}{2}\left(\frac{i\pi}{l}\right)+\frac{b\mu(c+d_t)}{2}\left(\frac{i\pi}{l}\right)^3\right]C_{ut}(i) \\
&+\left[\frac{b(c+d_t)}{2}\left(\frac{i\pi}{l}\right)+\frac{b\mu(c+d_t)}{2}\left(\frac{i\pi}{l}\right)^3\right]C_{ub}(i) \\
&+\left[\begin{array}{l}\dfrac{c}{G_c}E_tI_t\left(\dfrac{i\pi}{l}\right)^4 \\ +E_tI_t\left(\dfrac{\mu c}{G_c}+\dfrac{c^3}{12E_c}\right)\left(\dfrac{i\pi}{l}\right)^6 \\ +\dfrac{b\mu E_c}{G_c}\left(\dfrac{i\pi}{l}\right)^2 \\ +\dfrac{b\mu E_c}{c}\left(\dfrac{\mu c}{G_c}+\dfrac{c^3}{12E_c}\right)\left(\dfrac{i\pi}{l}\right)^4 \\ +\dfrac{b(c+d_t)^2}{4}\left(\dfrac{i\pi}{l}\right)^2 \\ +\dfrac{b\mu(c+d_t)^2}{4}\left(\dfrac{i\pi}{l}\right)^4 \\ +\dfrac{bE_c}{G_c}+\dfrac{bE_c}{c}\left(\dfrac{\mu c}{G_c}+\dfrac{c^3}{12E_c}\right)\left(\dfrac{i\pi}{l}\right)^2\end{array}\right]C_t(i) \\
&+\left[\begin{array}{l}-\dfrac{b\mu E_c}{G_c}\left(\dfrac{i\pi}{l}\right)^2 \\ -\dfrac{b\mu E_c}{c}\left(\dfrac{\mu c}{G_c}+\dfrac{c^3}{12E_c}\right)\left(\dfrac{i\pi}{l}\right)^4 \\ +\dfrac{b(c+d_t)(c+d_b)}{4}\left(\dfrac{i\pi}{l}\right)^2 \\ +\dfrac{b\mu(c+d_t)(c+d_b)}{4}\left(\dfrac{i\pi}{l}\right)^4 \\ -\dfrac{bE_c}{G_c}-\dfrac{bE_c}{c}\left(\dfrac{\mu c}{G_c}+\dfrac{c^3}{12E_c}\right)\left(\dfrac{i\pi}{l}\right)^2\end{array}\right]C_b(i) \\
&=\left[\begin{array}{l}\dfrac{c}{G_c}+\left(\dfrac{2\mu c}{G_c}+\dfrac{c^3}{12E_c}\right)\left(\dfrac{i\pi}{l}\right)^2 \\ +\mu\left(\dfrac{\mu c}{G_c}+\dfrac{c^3}{12E_c}\right)\left(\dfrac{i\pi}{l}\right)^4\end{array}\right]Q_i
\end{aligned} \tag{50}$$

$$\begin{aligned}
&-\left[\frac{b(c+d_b)}{2}\left(\frac{i\pi}{l}\right)+\frac{b\mu(c+d_b)}{2}\left(\frac{i\pi}{l}\right)^3\right]C_{ut}(i) \\
&+\left[\frac{b(c+d_b)}{2}\left(\frac{i\pi}{l}\right)+\frac{b\mu(c+d_b)}{2}\left(\frac{i\pi}{l}\right)^3\right]C_{ub}(i)
\end{aligned} \tag{51}$$

$$+\begin{bmatrix} -\dfrac{b\mu E_c}{G_c}\left(\dfrac{i\pi}{l}\right)^2 \\ -\dfrac{b\mu E_c}{c}\left(\dfrac{\mu c}{G_c}+\dfrac{c^3}{12E_c}\right)\left(\dfrac{i\pi}{l}\right)^4 \\ +\dfrac{b(c+d_t)(c+d_b)}{4}\left(\dfrac{i\pi}{l}\right)^2 \\ +\dfrac{b\mu(c+d_t)(c+d_b)}{4}\left(\dfrac{i\pi}{l}\right)^4 \\ -\dfrac{bE_c}{G_c}-\dfrac{bE_c}{c}\left(\dfrac{\mu c}{G_c}+\dfrac{c^3}{12E_c}\right)\left(\dfrac{i\pi}{l}\right)^2 \end{bmatrix} C_t(i) + \begin{bmatrix} \dfrac{c}{G_c}E_bI_b\left(\dfrac{i\pi}{l}\right)^4 \\ +E_bI_b\left(\dfrac{\mu c}{G_c}+\dfrac{c^3}{12E_c}\right)\left(\dfrac{i\pi}{l}\right)^6 \\ +\dfrac{b\mu E_c}{G_c}\left(\dfrac{i\pi}{l}\right)^2 \\ +\dfrac{b\mu E_c}{c}\left(\dfrac{\mu c}{G_c}+\dfrac{c^3}{12E_c}\right)\left(\dfrac{i\pi}{l}\right)^4 \\ +\dfrac{b(c+d_b)^2}{4}\left(\dfrac{i\pi}{l}\right)^2 \\ +\dfrac{b\mu(c+d_b)^2}{4}\left(\dfrac{i\pi}{l}\right)^4 \\ +\dfrac{bE_c}{G_c}+\dfrac{bE_c}{c}\left(\dfrac{\mu c}{G_c}+\dfrac{c^3}{12E_c}\right)\left(\dfrac{i\pi}{l}\right)^2 \end{bmatrix} C_b(i) = 0 \tag{51}$$

Eqs. (48)-(51) can be written in a matrix form

$$\begin{bmatrix} a_{11} & a_{12} & a_{13} & a_{14} \\ a_{21} & a_{22} & a_{23} & a_{24} \\ a_{31} & a_{32} & a_{33} & a_{34} \\ a_{41} & a_{42} & a_{43} & a_{44} \end{bmatrix} \begin{bmatrix} C_t(i) \\ C_b(i) \\ C_{ut}(i) \\ C_{ub}(i) \end{bmatrix} = \begin{bmatrix} F \\ 0 \\ 0 \\ 0 \end{bmatrix} \tag{52}$$

The elements of the matrices are listed in the Appendix. By solving the matrix Eq. (52), w_t, w_b, u_{0t}, and u_{0b} can be determined.

4. Numerical results

To validate the presented theory with Frostig's high-order theory, Nonlocal parameter in the presented theory is considered zero, and mechanical and geometrical properties of the sandwich beam are chosen from Table 1. It is assumed that this sandwich beam is under the point load 'P = 490.322 N' which is applied to midspan of the upper skin. Table 2 presents the center deflection of the skins of this sandwich beam based on the proposed theory and Frostig's high-order theory. It is observed from Table 2 that center deflections of both theories are similar.

It is assumed that the nano-sandwich beam is composed of graphene skins and a polymer core. In this study, three cases with different loading types are investigated. In case (1) Point load 'P = 1 nN' is to the midspan of the upper skin and in cases (2) and (3) Distributed load 'q = 1nN/m' and sinusoidal load '$q = \sin(\pi x/l)nN/m$' are applied to this skin, respectively. In this study, considering 50 terms in the series solution leads to numerical convergence. Mechanical and geometrical properties of the nano-sandwich beam are presented in Table 3.

Tables 4-6 present the non-dimensional center deflection of skins of the nano-sandwich beam obtained by nonlocal high-order theory for various nonlocal parameters for cases (1), (2) and (3), respectively. Also, the deflection of skins for cases (1) and (2) are shown in Figs. 2 and 3, respectively. It is observed from these Figures and Tables that by increasing the nonlocal parameter, the deflections of the skins will be increased. Thus, the influence of small-scale effects is to increase the deflection of the nano-sandwich beam. Small-scale effects decrease the stiffness of material and thus increase the deflection.

It is also noticeable that by increasing the nonlocal

Table 1 Mechanical and geometrical properties of the sandwich beam (Frostig *et al*. 1992)

L	c	b	d_t	d_b	G_c	E_c	$E_t = E_b$
300 mm	18.55 mm	60 mm	0.5 mm	1 mm	0.020594 GPa	0.0514849 GPa	26.8898 GPa

Table 2 Center deflection of the skins of the sandwich beam subjected to point load 'P = 490.332 N' based on the proposed theory and Frostig's high-order theory

Center deflection (mm)	Ref. (Frostig *et al*. 1992)	Present study (μ = 0)
w_{t_center}	2.9712	2.9712
w_{b_center}	2.7816	2.7816

Table 3 Mechanical and geometrical properties of the nano-sandwich beam

L	c	b	$d_t = d_b$	G_c	E_c	$E_t=E_b$
75 nm	15 nm	15 nm	5 nm	2 GPa	4.88 GPa	660 GPa

Table 4 Non-dimensional center deflection of skins of the nano-sandwich beam subjected to point load 'P = 1 nN' for various nonlocal parameters [$\bar{w}_{center} = w_{center} \times 100 \times (EI / PL^3)$, ($E = E_t = E_b$), ($I = I_t = I_b$)

	μ = 0	μ = 2 nm^2	μ = 5 nm^2	μ = 10 nm^2
$\bar{w}_{t\_center}$	3.8914e-1	3.9168e-1	3.9548e-1	4.0178e-1
$\bar{w}_{b\_center}$	3.0146e-1	3.0273e-1	3.0464e-1	3.0785e-1

Table 5 Non-dimensional center deflection of skins of the nano-sandwich beam subjected to distributed load 'q = 1nN/m' for various nonlocal parameters [$\bar{w}_{center}$ = w_{center} × 100 × (El / qL^4), $(E = E_t = E_b)$, $(I = I_t = I_b)$

	μ = 0	μ = 2 nm^2	μ = 5 nm^2	μ = 10 nm^2
$\bar{w}_{t\_center}$	2.2852e-1	2.2917e-1	2.3015e-1	2.3178e-1
$\bar{w}_{b\_center}$	1.9090e-1	1.9161e-1	1.9268e-1	1.9445e-1

Table 6 Non-dimensional center deflection of skins of the nano-sandwich beam subjected to sinusoidal load 'q = $\sin(\pi x/l)$ nN/m' for various nonlocal parameters [$\bar{w}_{center}$ = w_{center} × 10^{11} × (El / L^4), $(E = E_t = E_b)$, $(I = I_t = I_b)$

	μ = 0	μ = 2 nm^2	μ = 5 nm^2	μ = 10 nm^2
$\bar{w}_{t\_center}$	1.8248e-1	1.8306e-1	1.8393e-1	1.8538e-1
$\bar{w}_{b\_center}$	1.5014e-1	1.5071e-1	1.5158e-1	1.5302e-1

parameter, the influence of small-scale effects will be increased and the deflections will be increased more. This can be shown by introducing a parameter called deflection increase percentage (DIP). Deflection increase percentage (DIP) is defined as

$$DIP = \frac{|w_{nonlocal}| - |w_{local}|}{|w_{local}|} \times 100 \tag{53}$$

Figs. 4 and 5 show the variation of DIP for midspan of the skins against the nonlocal parameter for cases (1) and (2), respectively. According to these figures, by increasing the nonlocal parameter, the DIP for midspan of the skins increases.

For a clearer comparison between deflection of the upper and lower skins, Figs. 6 and 7 are presented for cases (1) and (2) with μ = 4 nm^2, respectively. These figures show

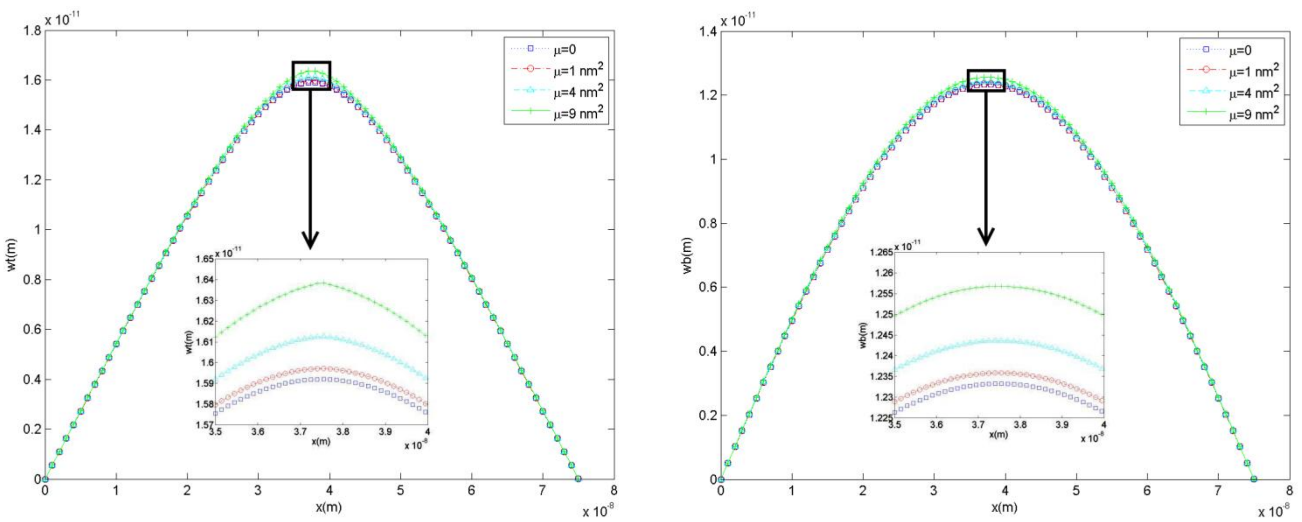

(a) Upper skin (b) Lower skin

Fig. 2 Deflection of the skins of the nano-sandwich beam under the point load 'P = 1 nN' for various nonlocal parameters

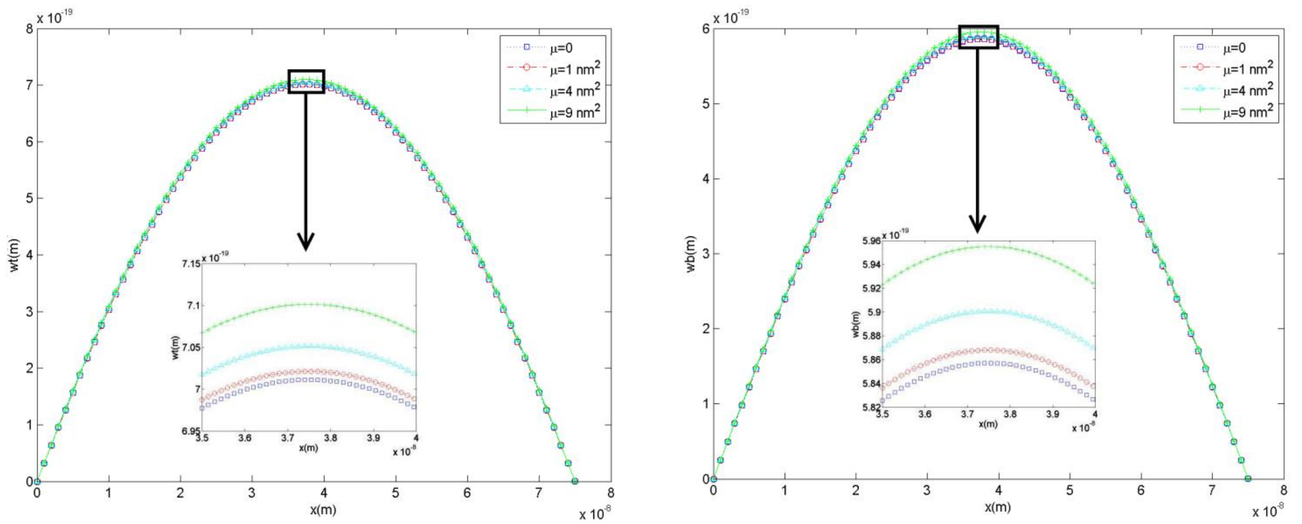

(a) Upper skin (b) Lower skin

Fig. 3 Deflection of the skins of nano-sandwich beam under the distributed load 'q = 1 nN/m' for various nonlocal parameters

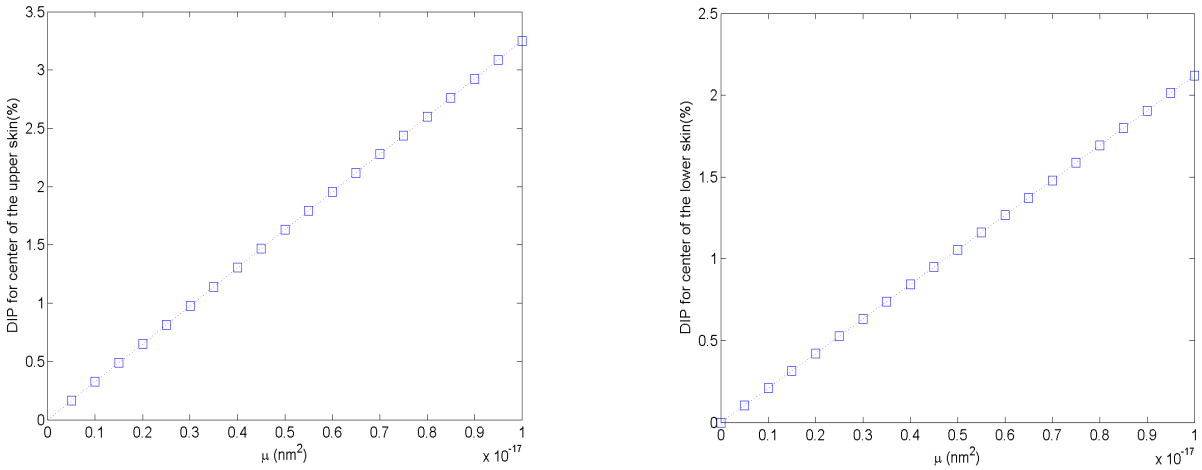

(a) Upper skin (b) Lower skin

Fig. 4 Variation of DIP for midspan of the skins of the nano-sandwich beam under the point load 'P = 1 nN' with the nonlocal parameter

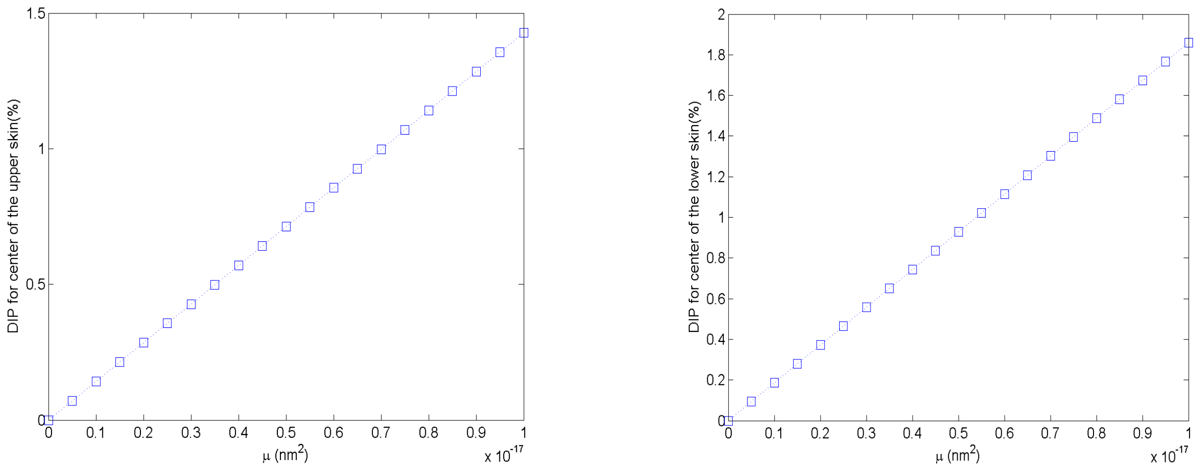

(a) Upper skin (b) Lower skin

Fig. 5 Variation of DIP for midspan of the skins of the nano-sandwich beam under the distributed load 'q = 1 nN/m' with the nonlocal parameter

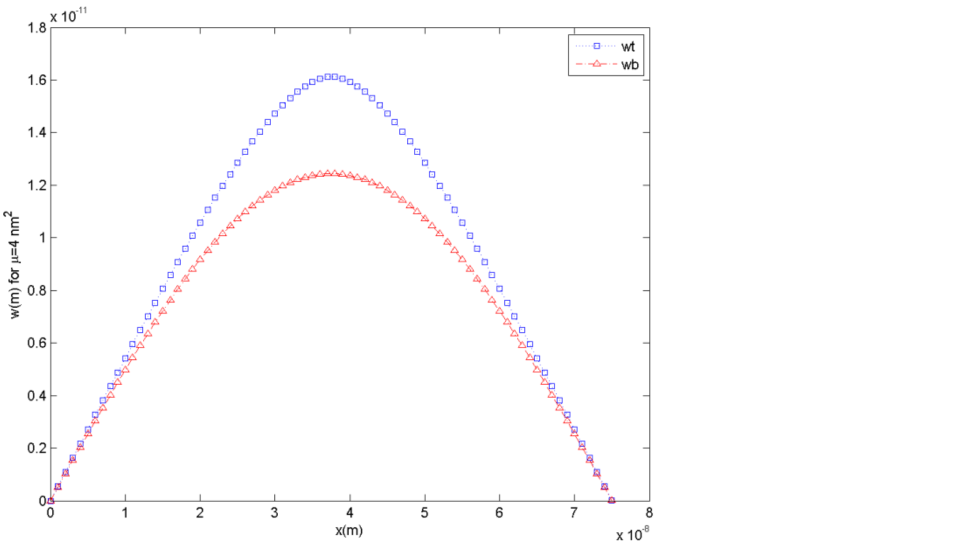

Fig. 6 Deflection of the upper and lower skins of the nano-sandwich beam under the point load 'P = 1 Nn' for μ = 4 nm^2

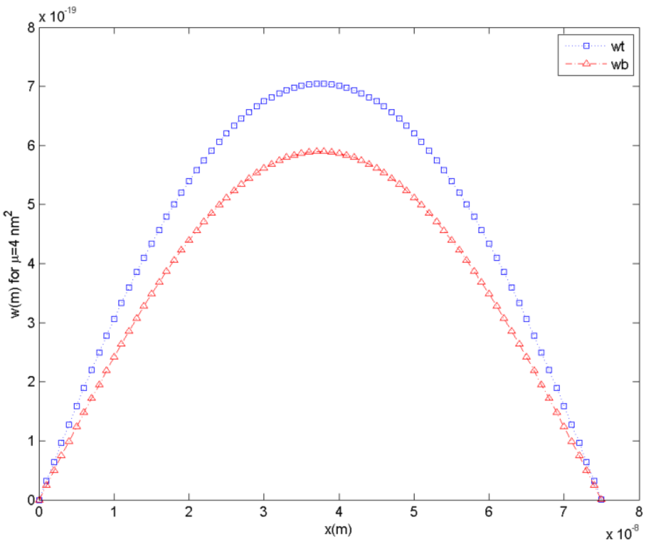

Fig. 7 Deflection of the upper and lower skins of the nano-sandwich beam under the distributed load ‘q = 1 nN/m’ for μ = 4 nm^2

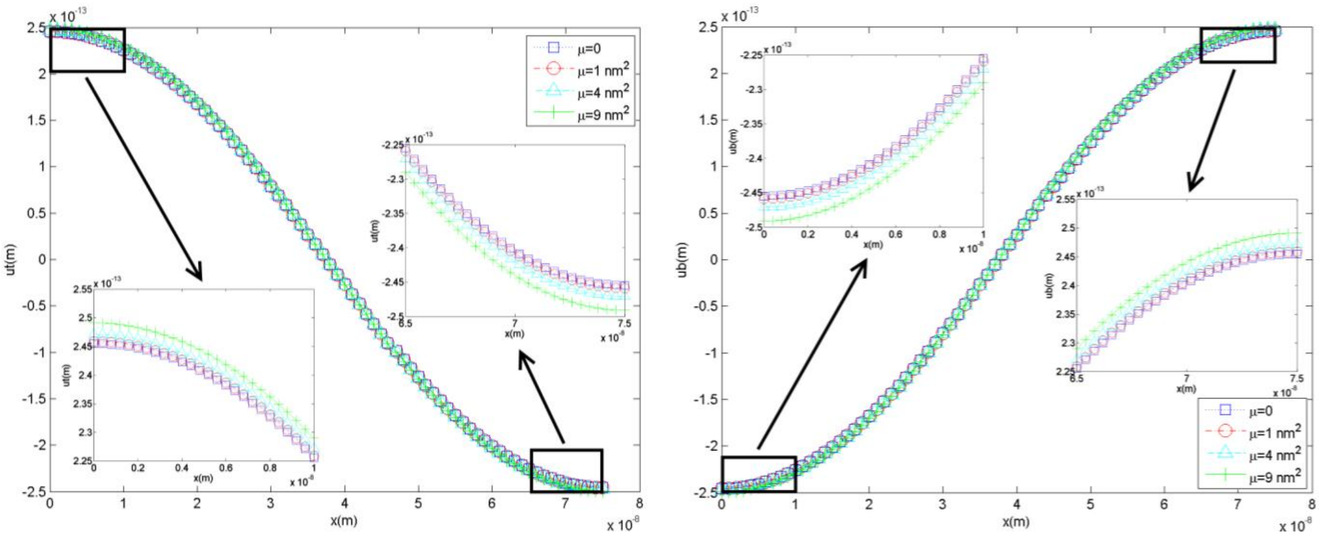

(a) Upper skin

(b) Lower skin

Fig. 8 Horizontal displacement of the skins of the nano-sandwich beam under the point load ‘P = 1 nN’ for various nonlocal parameters

that the deflection of the upper skin is greater than that of the lower skin. This behavior is due to the presence of the flexible core between the skins. This flexible core has nonlinear displacement fields, and absorbs some of the energy caused by loading. Thus, less energy will be transferred to the lower skin.

Figs. 8 and 9 present horizontal displacement of the skins of the nano-sandwich beam for various nonlocal parameters, for cases (1) and (2), respectively. It is concluded from these figures that by including the small-scale effects in the analysis, horizontal displacement of the skins will also be increased. It is also noticeable that by increasing the nonlocal parameter, horizontal displacement of the skins will be increased.

For the first and second cases, the effect of Young’s modulus of the core on the deflection of the upper and lower skins for various nonlocal parameters is shown in Figs. 10-13. By decreasing Young’s modulus of the core, i.e., by increasing E / E_c (E_t = E_b = E), the core will become more flexible and thus the deflection of the upper skin will be increased. However, by softening the core, the deflection of the lower skin will become smaller, since most of the deformation will occur in the core.

Figs. 14 and 15 show the effect of Young’s modulus of the core on the DIP for midspan of the skins of the nano-sandwich beam for cases (1) and (2), respectively. According to Fig. 14(a), by increasing E_c to E / E_c ≈ 71.5, the DIP for the midspan of the upper skin will be increased for various nonlocal parameters, i.e., the influence of the small-scale effects on deflection of the upper skin will be increased. By increasing E_c further from E / E_c ≈ 71.5, the DIP for the midspan of the upper skin will be slightly

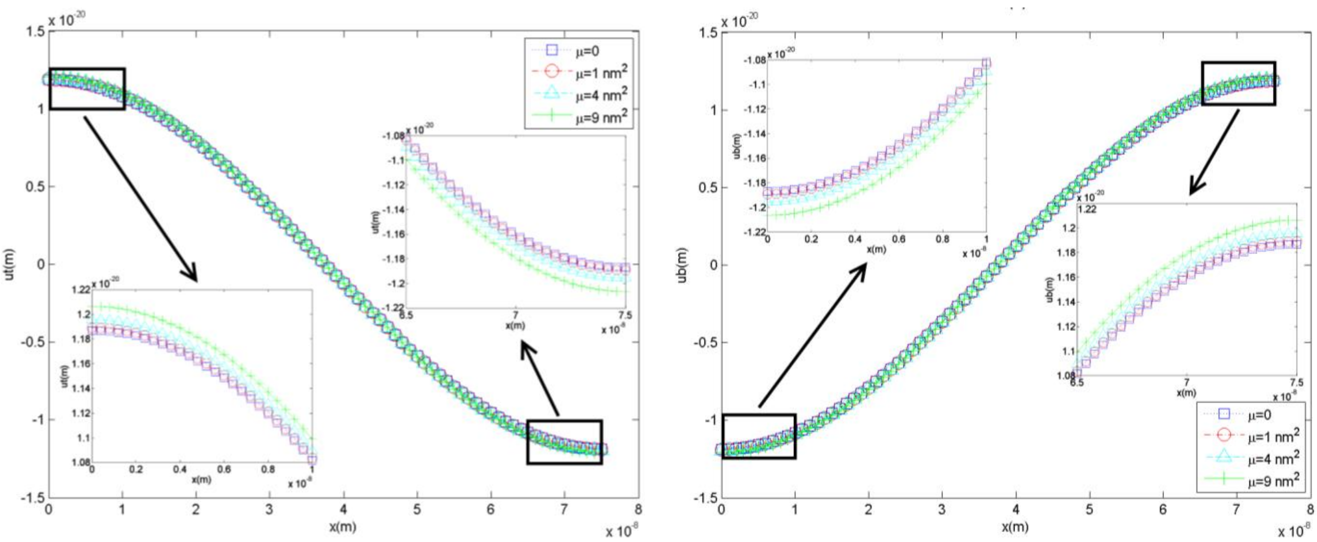

(a) Upper skin (b) Lower skin

Fig. 9 Horizontal displacement of the skins of nano-sandwich beam under the distributed load 'q = 1 nN/m' for various nonlocal parameters

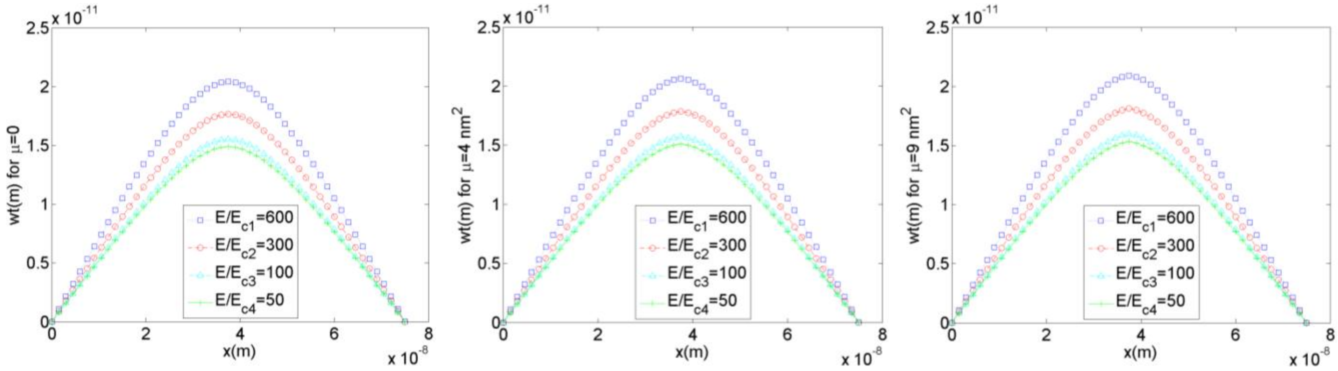

(a) μ = 0 (b) μ = 4 nm^2 (c) μ = 9 nm^2

Fig. 10 The effect of Young's modulus of the core on deflection of the upper skin of the nano-sandwich beam under the point load 'P = 1 nN'

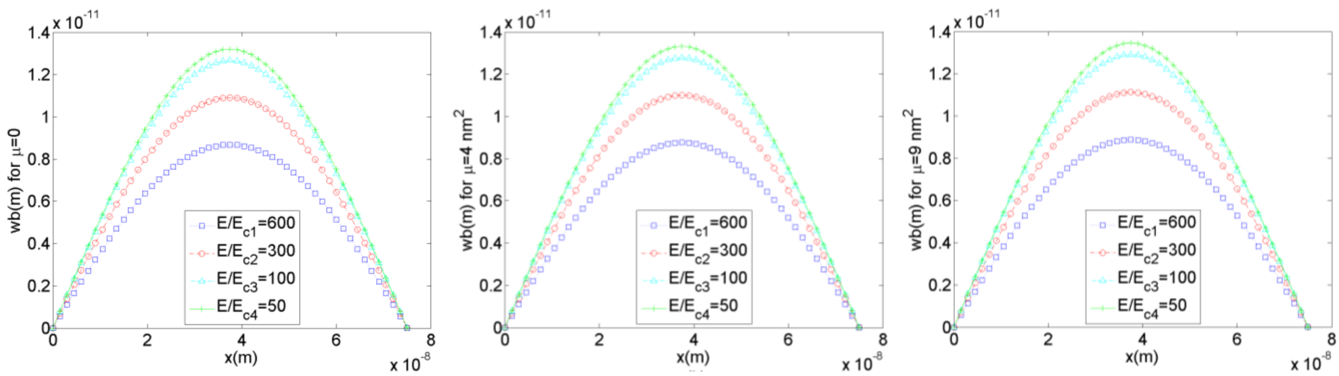

(a) μ = 0 (b) μ = 4 nm^2 (c) μ = 9 nm^2

Fig. 11 The effect of Young's modulus of the core on deflection of the lower skin of the nano-sandwich beam under the point load 'P =1nN'

decreased, i.e., the influence of the small-scale effects on deflection of the upper skin will be slightly decreased. Also, Fig. 14(b) shows that by increasing E_c to E / E_c ≈ 143.8, the influence of the small-scale effects on deflection of the lower skin will be decreased for various nonlocal parameters and by increasing E_c further from E / E_c ≈ 143.8,

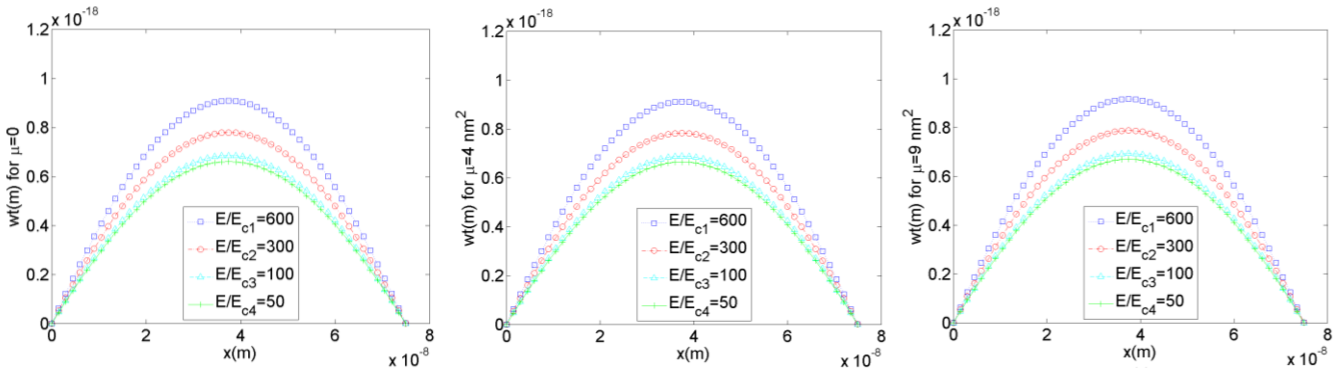

(a) $\mu = 0$ (b) $\mu = 4\ nm^2$ (c) $\mu = 9\ nm^2$

Fig. 12 The effect of Young's modulus of the core on deflection of the upper skin of the nano-sandwich beam under the distributed load '$q = 1\ nN/m$'

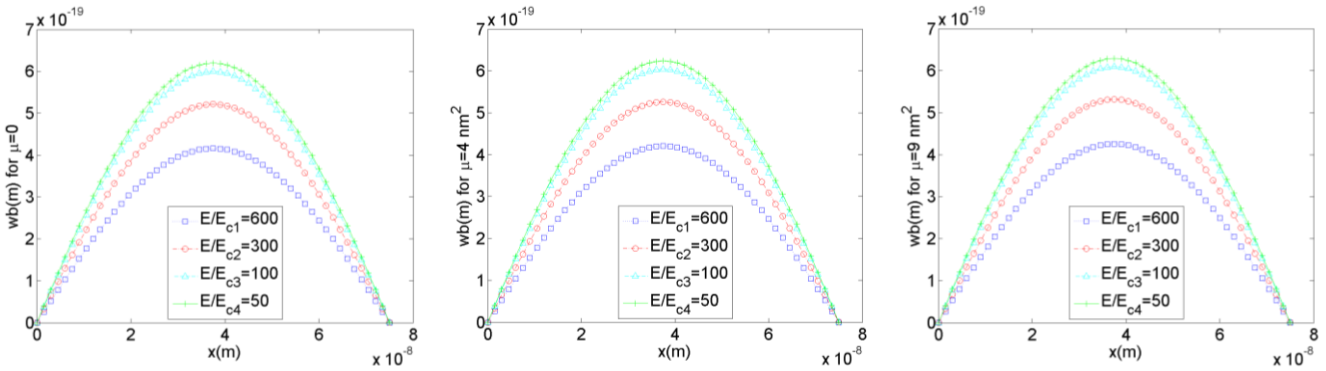

(a) $\mu = 0$ (b) $\mu = 4\ nm^2$ (c) $\mu = 9\ nm^2$

Fig. 13 The effect of Young's modulus of the core on deflection of the lower skin of the nano-sandwich beam under the distributed load '$q = 1nN/m$'

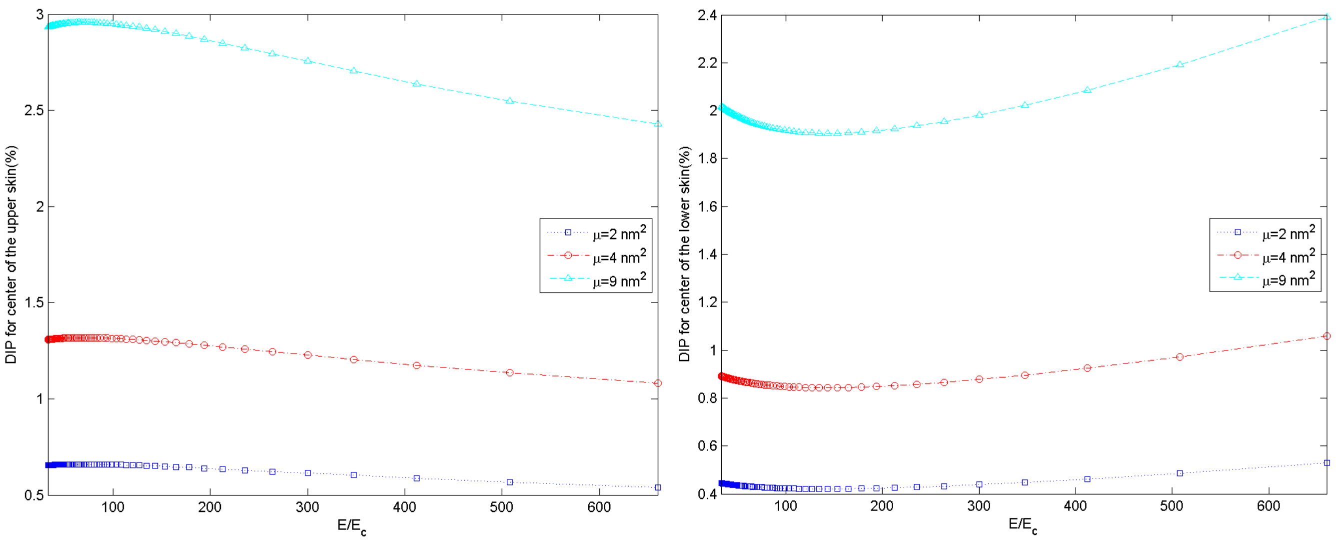

(a) Upper skin (b) Lower skin

Fig. 14 Variation of DIP for midspan of the skins of the nano-sandwich beam under the point load '$P = 1\ nN$' with E / E_c for various nonlocal parameters

this influence will be slightly increased. Fig. 15(a) shows that in case (2), by increasing the Young's modulus of the core, the influence of the small-scale effects on deflection of the upper skin will be increased for various nonlocal parameters. Also, according to Fig. 15(b), by increasing Young's modulus of the core, the influence of the small-

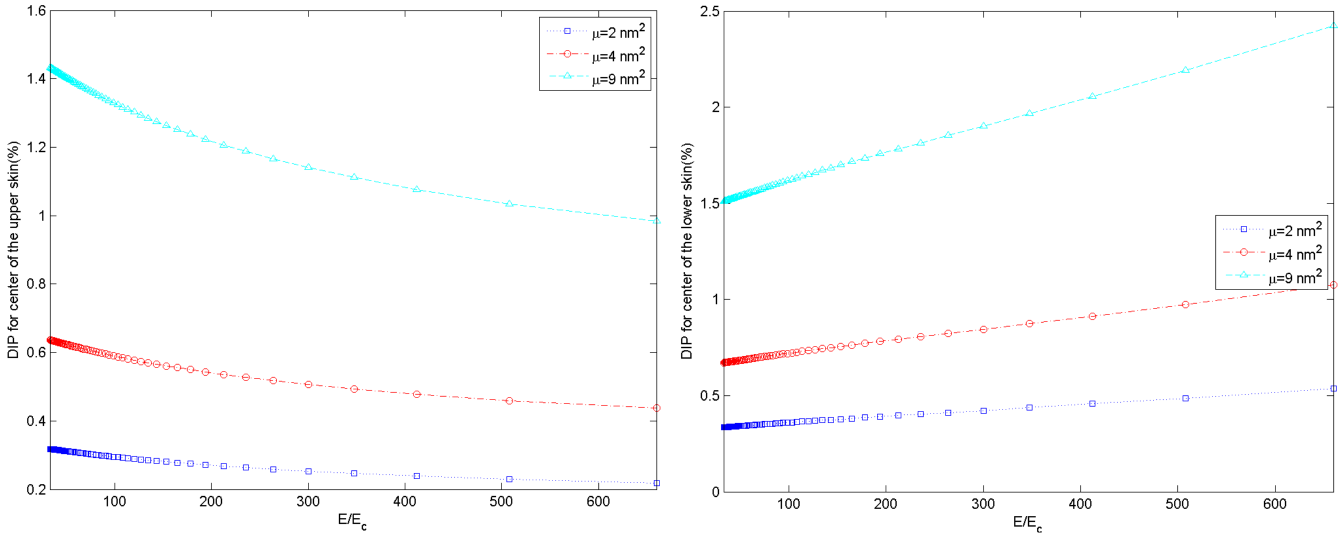

(a) Upper skin (b) Lower skin

Fig. 15 Variation of DIP for midspan of the skins of the nano-sandwich beam under the distributed load 'q = 1 nN/m' with E / E_c for various nonlocal parameters

Table 7 Non-dimensional center deflection of the skins of the nano-sandwich beam subjected to point load 'P = 1 nN' for various length to height ratios and nonlocal parameters [$\overline{w}_{center} = w_{center} \times 100 \times (E_t I_t / PL^3)$]

		L/h								
μ (nm^2)	Center deflection	5	10	15	20	25	30	35	40	45
0	$\overline{w}_{t\_center}$	1.79072e-1	6.57207e-2	4.17628e-2	3.30012e-2	2.88541e-2	2.65704e-2	2.51806e-2	2.42726e-2	2.36469e-2
	$\overline{w}_{b\_center}$	1.60206e-1	6.33625e-2	4.10640e-2	3.27064e-2	2.87032e-2	2.64831e-2	2.51256e-2	2.42357e-2	2.36210e-2
1	$\overline{w}_{t\_center}$	1.79356e-1	6.57581e-2	4.17744e-2	3.30064e-2	2.88569e-2	2.65721e-2	2.51817e-2	2.42733e-2	2.36474e-2
	$\overline{w}_{b\_center}$	1.60353e-1	6.33830e-2	4.10707e-2	3.27095e-2	2.87049e-2	2.64841e-2	2.51263e-2	2.42362e-2	2.36214e-2
4	$\overline{w}_{t\_center}$	1.80205e-1	6.58702e-2	4.18094e-2	3.30219e-2	2.88652e-2	2.65771e-2	2.51850e-2	2.42756e-2	2.36491e-2
	$\overline{w}_{b\_center}$	1.60796e-1	6.34445e-2	4.10907e-2	3.27187e-2	2.87100e-2	2.64873e-2	2.51285e-2	2.42378e-2	2.36225e-2
9	$\overline{w}_{t\_center}$	1.81615e-1	6.60564e-2	4.18675e-2	3.30476e-2	2.88790e-2	2.65854e-2	2.51905e-2	2.42795e-2	2.36519e-2
	$\overline{w}_{b\_center}$	1.61539e-1	6.35476e-2	4.11243e-2	3.27342e-2	2.87186e-2	2.64926e-2	2.51321e-2	2.42403e-2	2.36244e-2

Table 8 Non-dimensional center deflection of the skins of the nano-sandwich beam subjected to distributed load 'q = 1 nN/m' for various length to height ratios and nonlocal parameters [$\overline{w}_{center} = w_{center} \times 100 \times (E_t I_t / qL^4)$]

		L/h								
μ (nm^2)	Center deflection	5	10	15	20	25	30	35	40	45
0	$\overline{w}_{t\_center}$	1.02478e-1	3.73866e-2	2.41555e-2	1.94315e-2	1.72285e-2	1.60275e-2	1.53019e-2	1.48303e-2	1.45067e-2
	$\overline{w}_{b\_center}$	9.81117e-2	3.71161e-2	2.41021e-2	1.94146e-2	1.72216e-2	1.60242e-2	1.53001e-2	1.48292e-2	1.45061e-2
1	$\overline{w}_{t\_center}$	1.02535e-1	3.73918e-2	2.41571e-2	1.94322e-2	1.72289e-2	1.60278e-2	1.53021e-2	1.48304e-2	1.45068e-2
	$\overline{w}_{b\_center}$	9.81685e-2	3.71213e-2	2.41036e-2	1.94153e-2	1.72220e-2	1.60244e-2	1.53003e-2	1.48294e-2	1.45062e-2
4	$\overline{w}_{t\_center}$	1.02706e-1	3.74075e-2	2.41617e-2	1.94343e-2	1.72302e-2	1.60286e-2	1.53026e-2	1.48309e-2	1.45072e-2
	$\overline{w}_{b\_center}$	9.83387e-2	3.71369e-2	2.41082e-2	1.94174e-2	1.72232e-2	1.60252e-2	1.53008e-2	1.48298e-2	1.45065e-2
9	$\overline{w}_{t\_center}$	1.02990e-1	3.74335e-2	2.41693e-2	1.94379e-2	1.72322e-2	1.60299e-2	1.53036e-2	1.48316e-2	1.45077e-2
	$\overline{w}_{b\_center}$	9.86226e-2	3.71629e-2	2.41159e-2	1.94209e-2	1.72253e-2	1.60266e-2	1.53018e-2	1.48305e-2	1.45070e-2

Table 9 Non-dimensional center deflection of the skins of the nano-sandwich beam subjected to sinusoidal load ‘$q = \sin(\pi x/l)\ nN/m$’ for various length to height ratios and nonlocal parameters [$\bar{w}_{center} = w_{center} \times 10^{11} \times (E_t I_t / L^4)$)

		L/h								
$\mu\ (nm^2)$	Center deflection	5	10	15	20	25	30	35	40	45
0	$\bar{w}_{t\_center}$	8.20972e-2	2.99174e-2	1.92642e-2	1.54493e-2	1.36677e-2	1.26958e-2	1.21082e-2	1.17263e-2	1.14642e-2
	$\bar{w}_{b\_center}$	7.77875e-2	2.96469e-2	1.92107e-2	1.54323e-2	1.36608e-2	1.26924e-2	1.21064e-2	1.17253e-2	1.14636e-2
1	$\bar{w}_{t\_center}$	8.21475e-2	2.99221e-2	1.92655e-2	1.54499e-2	1.36681e-2	1.26960e-2	1.21084e-2	1.17264e-2	1.14643e-2
	$\bar{w}_{b\_center}$	7.78378e-2	2.96516e-2	1.92121e-2	1.54330e-2	1.36612e-2	1.26927e-2	1.21066e-2	1.17254e-2	1.14636e-2
4	$\bar{w}_{t\_center}$	8.22984e-2	2.99362e-2	1.92696e-2	1.54517e-2	1.36691e-2	1.26967e-2	1.21089e-2	1.17268e-2	1.14646e-2
	$\bar{w}_{b\_center}$	7.79887e-2	2.96657e-2	1.92161e-2	1.54348e-2	1.36622e-2	1.26933e-2	1.21071e-2	1.17257e-2	1.14639e-2
9	$\bar{w}_{t\_center}$	8.25500e-2	2.99597e-2	1.92763e-2	1.54547e-2	1.36709e-2	1.26978e-2	1.21096e-2	1.17274e-2	1.14650e-2
	$\bar{w}_{b\_center}$	7.82402e-2	2.96892e-2	1.92229e-2	1.54378e-2	1.36639e-2	1.26944e-2	1.21078e-2	1.17263e-2	1.14644e-2

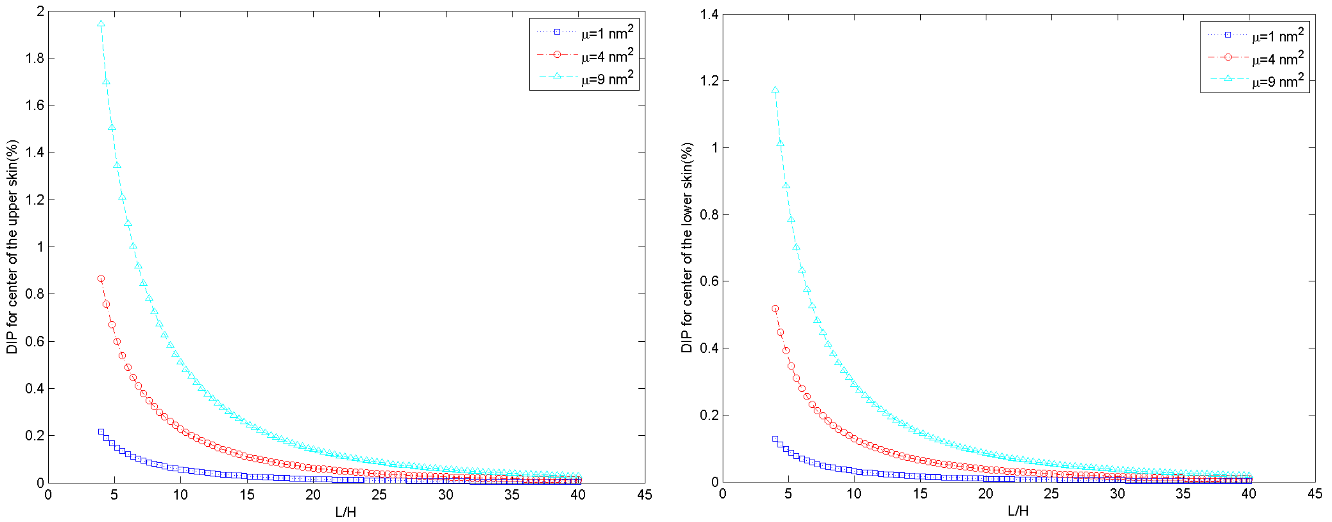

(a) Upper skin (b) Lower skin

Fig. 16 Variation of DIP for midspan of the skins of the nano-sandwich beam under the point load ‘$P = 1\ nN$’ with length to height ratio for various nonlocal parameters

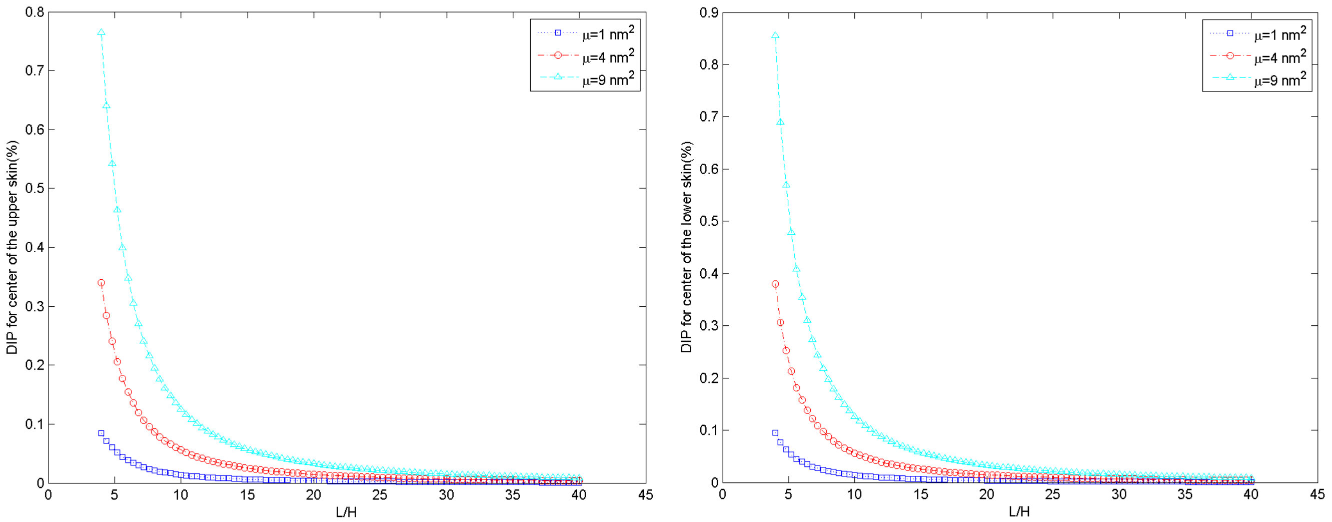

(a) Upper skin (b) Lower skin

Fig. 17 Variation of DIP for midspan of the skins of the nano-sandwich beam under the distributed load ‘$q = 1\ nN/m$’ with length to height ratio for various nonlocal parameters scale effects on the deflection of the lower skin will be decreased for various nonlocal parameters.

Tables 7, 8 and 9 present the non-dimensional center deflection of the skins of the nano-sandwich beam for various length to height ratios and nonlocal parameters for cases (1), (2) and (3), respectively. It is observed that by increasing length to height ratio of the nano-sandwich beam, the non-dimensional center deflection of the skins will be decreased.

Figs. 16 and 17 show the effect of length to height ratio of the nano-sandwich beam on the DIP for midspan of the skins for cases (1) and (2), respectively. It can be seen that by increasing the length to height ratio, DIP for midspan of the skins will be decreased, i.e., the influence of the small-scale effects on deflection of the skins will be decreased.

5. Conclusions

In this paper, bending analysis of the nano-sandwich beam with a flexible core based on nonlocal high order theory is studied. The skins of this nanostructure are thin and thus classical beam theory is applied to them. The core is flexible in the vertical direction and its longitudinal and vertical displacement fields are nonlinear. The governing equations are derived by using Hamilton's principle and Eringen's nonlocal elasticity. Navier's method is used to solve the bending behavior of a simply-supported nano-sandwich beam. Numerical results for this case are presented and the effect of nonlocal parameter, Young's modulus of the core and length to height ratio on the deflection of the nano-sandwich beam is investigated.

- It is concluded that by including the small-scale effects, the deflection of the skins is increased and by increasing the nonlocal parameter, the influence of small-scale effects on the deflections is increased.
- It is seen that by decreasing Young's modulus of the core, deflection of the upper skin is increased whereas deflection of the lower skin is decreased.
- It is observed that by increasing length to height ratio, the non-dimensional center deflection of the skins will be decreased.
- The effect of Young's modulus of the core and length to height ratio on the influence of the nonlocal parameter on deflection of the nano-sandwich beam is also studied. For case (1), it is observed that by increasing Young's modulus of the core to a certain value, the influence of the small-scale effects on deflection of the upper skin is increased, and by increasing Young's modulus of the core further from that value, this influence is slightly reduced. Also, it can be seen that by increasing Young's modulus of the core to a certain value, the influence of nonlocal parameter on deflection of the lower skin is decreased, and by increasing Young's modulus of the core further from that value, this influence is slightly increased. For case (2), it is concluded that by increasing Young's modulus of the core, the influence of the small-scale effects on deflection of the upper skin is increased, and the influence of the small-scale effects on deflection of the lower skin is reduced.
- The effect of length to height ratio on the influence of the nonlocal parameter on deflection of the nano-sandwich beam is investigated. It is noted that increasing length to height ratio of the nano-sandwich beam reduces the influence of nonlocal parameter on deflection of the skins.

References

Ahouel, M., Houari, M.S.A., Bedia, E.A. and Tounsi, A. (2016), "Size-dependent mechanical behavior of functionally graded trigonometric shear deformable nanobeams including neutral surface position concept", *Steel Compos. Struct., Int. J.*, **20**(5), 963-981.

Belkorissat, I., Houari, M.S.A., Tounsi, A., Bedia, E.A. and Mahmoud, S.R. (2015), "On vibration properties of functionally graded nano-plate using a new nonlocal refined four variable model", *Steel Compos. Struct., Int. J.*, **18**(4), 1063-1081.

Bennai, R., Atmane, H.A. and Tounsi, A. (2015), "A new higher-order shear and normal deformation theory for functionally graded sandwich beams", *Steel Compos. Struct., Int. J.*, **19**(3), 521-546.

Bouchafa, A., Bouiadjra, M.B., Houari, M.S.A. and Tounsi, A. (2015), "Thermal stresses and deflections of functionally graded sandwich plates using a new refined hyperbolic shear deformation theory", *Steel Compos. Struct., Int. J.*, **18**(6), 1493-1515.

Bounouara, F., Benrahou, K.H., Belkorissat, I. and Tounsi, A. (2016), "A nonlocal zeroth-order shear deformation theory for free vibration of functionally graded nanoscale plates resting on elastic foundation", *Steel Compos. Struct., Int. J.*, **20**(2), 227-249.

Chaht, F.L., Kaci, A., Houari, M.S.A., Tounsi, A., Bég, O.A. and Mahmoud, S.R. (2015), "Bending and buckling analyses of functionally graded material (FGM) size-dependent nanoscale beams including the thickness stretching effect", *Steel Compos. Struct., Int. J.*, **18**(2), 425-442.

Eichenfield, M., Camacho, R., Chan, J., Vahala, K.J. and Painter, O. (2009), "A picogram-and nanometre-scale photonic-crystal optomechanical cavity", *Nature*, **459**(7246), 550-555.

Emam, S.A. (2013), "A general nonlocal nonlinear model for buckling of nanobeams", *Appl. Math. Model.*, **37**(10), 6929-6939.

Frostig, Y. (2014), "Non-linear behavior of a face-sheet debonded sandwich panel–Thermal effects", *Int. J. Non-Linear Mech.*, **64**, 1-25.

Frostig, Y., Baruch, M., Vilnay, O. and Sheinman, I. (1992), "High-order theory for sandwich-beam behavior with transversely flexible core", *J. Eng. Mech.*, **118**(5), 1026-1043.

Frostig, Y., Phan, C.N. and Kardomateas, G.A. (2013), "Free vibration of unidirectional sandwich panels, Part I: Compressible core", *J. Sandw. Struct. Mater.*, **45**(4), 377-411.

Ghavanloo, E. and Fazelzadeh, S.A. (2013), "Radial vibration of free anisotropic nanoparticles based on nonlocal continuum mechanics", *Nanotechnology*, **24**(7), 075702.

Hamidi, A., Houari, M.S.A., Mahmoud, S.R. and Tounsi, A. (2015), "A sinusoidal plate theory with 5-unknowns and stretching effect for thermomechanical bending of functionally graded sandwich plates", *Steel Compos. Struct., Int. J.*, **18**(1), 235-253.

Hayati, H., Hosseini, S.A. and Rahmani, O. (2016), "Coupled twist–bending static and dynamic behavior of a curved single-walled carbon nanotube based on nonlocal theory", *Microsyst.*

Technol., **23**(7), 2393-2401.

Hosseini, S. and Rahmani, O. (2016), "Surface effects on buckling of double nanobeam system based on nonlocal Timoshenko model", *Int*. *J*. *Struct*. *Stabil*. *Dyn*., **16**(10), 1550077.

Jandaghian, A.A. and Rahmani, O. (2015), "On the buckling behavior of piezoelectric nanobeams: An exact solution", *J*. *Mech*. *Sci*. *Technol*., **29**(8), 3175-3182.

Khalili, S.M.R., Rahmani, O., Malekzadeh Fard, K. and Thomsen, O.T. (2014), "High-order modeling of circular cylindrical composite sandwich shells with a transversely compliant core subjected to low velocity impact", *Mech*. *Adv*. *Mater*. *Struct*., **21**(8), 680-695.

Lashkari, M.J. and Rahmani, O. (2016), "Bending behavior of sandwich structures with flexible functionally graded core based on high-order sandwich panel theory", *Meccanica*, **51**(5), 1093-1112.

Miandoab, E.M., Yousefi-Koma, A. and Pishkenari, H.N. (2015), "Nonlocal and strain gradient based model for electrostatically actuated silicon nano-beams", *Microsyst*. *Technol*., **21**(2), 457-464.

Murmu, T. and Adhikari, S. (2010), "Nonlocal transverse vibration of double-nanobeam-systems", *J*. *Appl*. *Phys*., **108**(8), 083514.

Murmu, T. and Adhikari, S. (2011a), "Axial instability of double-nanobeam-systems", *Phys*. *Lett*. *A*, **375**(3), 601-608.

Murmu, T. and Adhikari, S. (2011b), "Nonlocal vibration of bonded double-nanoplate-systems", *Compos*. *Part B*: *Eng*., **42**(7), 1901-1911.

Murmu, T., Sienz, J., Adhikari, S. and Arnold, C. (2011), "Nonlocal buckling behavior of bonded double-nanoplate-systems", *J*. *Appl*. *Phys*., **110**(8), 084316.

Najafi, F., Shojaeefard, M.H. and Googarchin, H.S. (2016), "Nonlinear low-velocity impact response of functionally graded plate with nonlinear three-parameter elastic foundation in thermal field", *Compos*. *Part B*: *Eng*., **107**, 123-140.

Najafi, F., Shojaeefard, M.H. and Googarchin, H.S. (2017), "Nonlinear dynamic response of FGM beams with Winkler–Pasternak foundation subject to noncentral low velocity impact in thermal field", *Compos*. *Struct*., **167**, 132-143.

Nguyen, N.T., Kim, N.I. and Lee, J. (2014), "Analytical solutions for bending of transversely or axially FG nonlocal beams", *Steel Compos*. *Struct*., *Int*. *J*., **17**(5), 641-665.

Patti, A., Barretta, R., de Sciarra, F.M., Mensitieri, G., Menna, C. and Russo, P. (2015), "Flexural properties of multi-wall carbon nanotube/polypropylene composites: Experimental investigation and nonlocal modeling", *Compos*. *Struct*., **131**, 282-289.

Phan, C.N., Frostig, Y. and Kardomateas, G.A. (2012a), "Analysis of sandwich beams with a compliant core and with in-plane rigidity—extended high-order sandwich panel theory versus elasticity", *J*. *Appl*. *Mech*., **79**(4), 041001.

Phan, C.N., Kardomateas, G.A. and Frostig, Y. (2012b), "Global buckling of sandwich beams based on the extended high-order theory", *AIAA Journal*, **50**(8), 1707-1716.

Pourseifi, M., Rahmani, O. and Hoseini, S.A.H. (2015), "Active vibration control of nanotube structures under a moving nanoparticle based on the nonlocal continuum theories", *Meccanica*, **50**(5), 1351-1369.

Rahmani, O. (2014), "On the flexural vibration of pre-stressed nanobeams based on a nonlocal theory", *Acta Phys*. *Pol*. *A*, **125**(2), 532.

Rahmani, O., Khalili, S.M.R. and Thomsen, O.T. (2012), "A high-order theory for the analysis of circular cylindrical composite sandwich shells with transversely compliant core subjected to external loads", *Composite Structures*, **94**(7), 2129-2142.

Rahmani, O., Hosseini, S.A.H. and Hayati, H. (2016), "Frequency analysis of curved nano-sandwich structure based on a nonlocal model", *Modern Physics Letters B*, **30**(10), 1650136.

Reddy, J. (2007), "Nonlocal theories for bending, buckling and vibration of beams", *Int*. *J*. *Eng*. *Sci*., **45**(2), 288-307.

Shojaeefard, M.H., Googarchin, H.S., Ghadiri, M. and Mahinzare, M. (2017), "Micro temperature-dependent FG porous plate: free vibration and thermal buckling analysis using modified couple stress theory with CPT and FSDT", *Appl*. *Math*. *Model*., **50**, 633-655.

Shojaeefard, M.H., Googarchin, H.S., Mahinzare, M. and Ghadiri, M. (2018), "Free vibration and critical angular velocity of a rotating variable thickness two-directional FG circular microplate", *Microsystem Technologies*, **24**(3), 1525-1543.

Simsek, M. (2011), "Forced vibration of an embedded single-walled carbon nanotube traversed by a moving load using nonlocal Timoshenko beam theory", *Steel Compos*. *Struct*., *Int*. *J*., **11**(1), 59-76.

Wang, Q. and Varadan, V.K. (2006), "Vibration of carbon nanotubes studied using nonlocal continuum mechanics", *Smart Mater*. *Struct*., **15**(2), 659.

Yuan, Z., Kardomateas, G.A. and Frostig, Y. (2015), "Finite element formulation based on the extended high-order sandwich panel theory", *AIAA Journal*, **53**(10), 3006-3015.

Zemri, A., Houari, M.S.A., Bousahla, A.A. and Tounsi, A. (2015), "A mechanical response of functionally graded nanoscale beam: an assessment of a refined nonlocal shear deformation theory beam theory", *Struct*. *Eng*. *Mech*., *Int*. *J*., **54**(4), 693-710.

CC

Appendix

The elements of the matrices in Eq. (52) are as followsG

$$a_{11}=\frac{c}{G_c}E_tI_t\left(\frac{i\pi}{l}\right)^4+E_tI_t\left(\frac{\mu c}{G_c}+\frac{c^3}{12E_c}\right)\left(\frac{i\pi}{l}\right)^6+\frac{b\mu E_c}{G_c}\left(\frac{i\pi}{l}\right)^2+\frac{b\mu E_c}{c}\left(\frac{\mu c}{G_c}+\frac{c^3}{12E_c}\right)\left(\frac{i\pi}{l}\right)^4$$
$$+\frac{b(c+d_t)^2}{4}\left(\frac{i\pi}{l}\right)^2+\frac{b\mu(c+d_t)^2}{4}\left(\frac{i\pi}{l}\right)^4+\frac{bE_c}{G_c}+\frac{bE_c}{c}\left(\frac{\mu c}{G_c}+\frac{c^3}{12E_c}\right)\left(\frac{i\pi}{l}\right)^2$$

$$a_{12}=-\frac{b\mu E_c}{G_c}\left(\frac{i\pi}{l}\right)^2-\frac{b\mu E_c}{c}\left(\frac{\mu c}{G_c}+\frac{c^3}{12E_c}\right)\left(\frac{i\pi}{l}\right)^4+\frac{b(c+d_t)(c+d_b)}{4}\left(\frac{i\pi}{l}\right)^2$$
$$+\frac{b\mu(c+d_t)(c+d_b)}{4}\left(\frac{i\pi}{l}\right)^4-\frac{bE_c}{G_c}-\frac{bE_c}{c}\left(\frac{\mu c}{G_c}+\frac{c^3}{12E_c}\right)\left(\frac{i\pi}{l}\right)^2$$

$$a_{13}=-\frac{b(c+d_t)}{2}\left(\frac{i\pi}{l}\right)-\frac{b\mu(c+d_t)}{2}\left(\frac{i\pi}{l}\right)^3$$

$$a_{14}=\frac{b(c+d_t)}{2}\left(\frac{i\pi}{l}\right)+\frac{b\mu(c+d_t)}{2}\left(\frac{i\pi}{l}\right)^3$$

$$a_{21}=-\frac{b\mu E_c}{G_c}\left(\frac{i\pi}{l}\right)^2-\frac{b\mu E_c}{c}\left(\frac{\mu c}{G_c}+\frac{c^3}{12E_c}\right)\left(\frac{i\pi}{l}\right)^4+\frac{b(c+d_t)(c+d_b)}{4}\left(\frac{i\pi}{l}\right)^2$$
$$+\frac{b\mu(c+d_t)(c+d_b)}{4}\left(\frac{i\pi}{l}\right)^4-\frac{bE_c}{G_c}-\frac{bE_c}{c}\left(\frac{\mu c}{G_c}+\frac{c^3}{12E_c}\right)\left(\frac{i\pi}{l}\right)^2$$

$$a_{22}=\frac{c}{G_c}E_bI_b\left(\frac{i\pi}{l}\right)^4+E_bI_b\left(\frac{\mu c}{G_c}+\frac{c^3}{12E_c}\right)\left(\frac{i\pi}{l}\right)^6+\frac{b\mu E_c}{G_c}\left(\frac{i\pi}{l}\right)^2+\frac{b\mu E_c}{c}\left(\frac{\mu c}{G_c}+\frac{c^3}{12E_c}\right)\left(\frac{i\pi}{l}\right)^4$$
$$+\frac{b(c+d_b)^2}{4}\left(\frac{i\pi}{l}\right)^2+\frac{b\mu(c+d_b)^2}{4}\left(\frac{i\pi}{l}\right)^4+\frac{bE_c}{G_c}+\frac{bE_c}{c}\left(\frac{\mu c}{G_c}+\frac{c^3}{12E_c}\right)\left(\frac{i\pi}{l}\right)^2$$

$$a_{23}=-\frac{b(c+d_b)}{2}\left(\frac{i\pi}{l}\right)-\frac{b\mu(c+d_b)}{2}\left(\frac{i\pi}{l}\right)^3$$

$$a_{24}=\frac{b(c+d_b)}{2}\left(\frac{i\pi}{l}\right)+\frac{b\mu(c+d_b)}{2}\left(\frac{i\pi}{l}\right)^3$$

$$a_{31}=\frac{b(c+d_t)}{2}\left(\frac{i\pi}{l}\right)+\frac{b\mu(c+d_t)}{2}\left(\frac{i\pi}{l}\right)^3$$

$$a_{32}=\frac{b(c+d_b)}{2}\left(\frac{i\pi}{l}\right)+\frac{b\mu(c+d_b)}{2}\left(\frac{i\pi}{l}\right)^3$$

$$a_{33}=-\frac{c}{G_c}E_tA_t\left(\frac{i\pi}{l}\right)^2-\left(\frac{\mu c}{G_c}+\frac{c^3}{12E_c}\right)E_tA_t\left(\frac{i\pi}{l}\right)^4-b-b\mu\left(\frac{i\pi}{l}\right)^2$$

$$a_{34}=b+b\mu\left(\frac{i\pi}{l}\right)^2$$